Journal of Virology

| Editor's Pick | Evolution | Full-Length Text

RSV F evolution escapes some monoclonal antibodies but does not strongly erode neutralization by human polyclonal sera

Cassandra A. L. Simonich,[1,2,3] Teagan E. McMahon,[1] Xiaohui Ju,[1] Timothy C. Yu,[1,4] Natalie Brunette,[5,6] Terry Stevens-Ayers,[7] Michael J. Boeckh,[7] Neil P. King,[5,6] Alexander L. Greninger,[7,8] Jesse D. Bloom[1,9]

AUTHOR AFFILIATIONS See affiliation list on p. 18.

ABSTRACT Vaccines and monoclonal antibodies targeting the respiratory syncytial virus (RSV) fusion protein (F) have recently begun to be widely used to protect infants and high-risk adults. Some other viral proteins evolve to erode polyclonal antibody neutralization and escape individual monoclonal antibodies. However, the impact of RSV F evolution on antibody neutralization is not yet thoroughly understood. Here, we develop an experimental system for measuring neutralization titers against RSV F using pseudotyped lentiviral particles. This system is easily adaptable to evaluate neutralization of relevant clinical strains. We apply this system to demonstrate that the natural evolution of RSV F leads to escape from some monoclonal antibodies, but at most modestly affects neutralization by polyclonal serum antibodies. Overall, our work sheds light on RSV antigenic evolution and describes a tool to measure the ability of antibodies and sera to neutralize contemporary RSV strains.

IMPORTANCE We describe an efficient approach to measure how antibodies inhibit infection by historical and recent human strains of respiratory syncytial virus (RSV). This approach is useful for understanding how viral evolution affects antibody immunity. We apply this approach to demonstrate that RSV evolution can escape some monoclonal antibodies, but polyclonal serum antibodies are less impacted by viral evolution. This information is relevant given the recent development of RSV preventative measures, including monoclonal antibodies and vaccines.

KEYWORDS RSV evolution, lentiviral pseudotyping, viral evolution, monoclonal antibodies, respiratory syncytial virus, RSV

Respiratory syncytial virus (RSV) is the leading cause of hospitalization for infants in the United States (1, 2) and can also cause severe illness and death in older adults and immunocompromised individuals (3–5). RSV has two surface glycoproteins, the fusion (F) and attachment (G) proteins. Neutralizing antibodies targeting the pre-fusion conformation of F are correlated with protection in humans (6–17). Therefore, recent efforts have focused on developing monoclonal antibodies or vaccines targeting F that can protect infants and high-risk adults. Three vaccines consisting of pre-fusion stabilized F have recently been approved for adults in the United States (10–12, 18), including one to protect infants via passive transfer of maternal antibodies (17, 19). Furthermore, the anti-F monoclonal antibody nirsevimab is now recommended for administration to infants in the United States during RSV season (20–22) and is licensed in several countries. Thus far, nirsevimab has shown around 83% effectiveness in preventing hospitalizations of infants (13, 16, 20, 23), and in the first year, demand for the antibody outstripped supply (24). Additional anti-F antibodies are now being developed for use in infants (9, 25). RSV is therefore the first virus for which a monoclonal antibody will be in

Editor Colin R. Parrish, Cornell University Baker Institute for Animal Health, Ithaca, New York, USA

Address correspondence to Jesse D. Bloom, jbloom@fredhutch.org.

J.D.B. consults for Apriori Bio, Invivyd, the Vaccine Company, GSK, and Pfizer. J.D.B. is an inventor on Fred Hutch-licensed patents related to deep mutational scanning of viral proteins. A.L.G. reports contract testing to UW from Abbott, Cepheid, Novavax, Pfizer, Janssen, and Hologic, as well as research support from Gilead, outside of the described work. M.J.B. has received research support from Merck, GSK, and AstraZeneca and consults for Merck, AstraZeneca, and Ivivyd. N.P.K. consults for AstraZeneca, and the King lab has received unrelated sponsored research agreements from Pfizer and GSK.

See the funding table on p. 19.

Received 20 March 2025
Accepted 6 June 2025
Published 3 July 2025

widespread sustained use in an appreciable fraction of the human population in some countries.

Some other human RNA viruses evolve to escape monoclonal antibodies and erode neutralization by polyclonal serum antibodies. For instance, vaccines for influenza virus and SARS-CoV-2 are updated annually to keep pace with viral evolution (26, 27), and over the last few years, SARS-CoV-2 escaped most clinically approved monoclonal antibodies (28, 29). The extent to which RSV F evolves to erode neutralization by either polyclonal or monoclonal antibodies is not yet fully understood. At the sequence level, RSV F is less variable than the surface proteins of influenza viruses or human coronaviruses (30–32). However, the potential for RSV to escape from monoclonal antibodies has long been recognized (33). One monoclonal antibody (suptavumab) failed in an expensive phase III clinical trial because it was escaped by mutations in circulating RSV-B strains (34). Additionally, recent studies have identified occasional strains with resistance mutations in F to nirsevimab (31, 32, 35–39).

Efforts to understand how RSV F's evolution impacts antibodies would benefit from assays to easily measure neutralization of F proteins from recent clinical strains. Currently, most common RSV neutralization assays utilize lab-adapted older strains that are not representative of recently circulating viruses (40, 41). Assays utilizing recent clinical strains are more challenging because the growth of clinical strains of RSV is challenging and yields low titers (42–47). Here, we developed a pseudotyping system to efficiently measure neutralizing antibody titers to the F proteins of historical and contemporary RSV strains. We show that RSV's natural evolution only modestly affects neutralization by polyclonal serum antibodies, but does lead to escape from some monoclonal antibodies.

RESULTS

Efficient pseudotyping of lentiviral particles with F and G from a variety of RSV strains

A widely used approach to study antibody neutralization targeting viral proteins involved in cell entry is to generate single-cycle infectious lentiviral particles that display the viral proteins on their surface and rely on the function of these proteins to infect target cells (48, 49). These "pseudotyped" viral particles can be used to study the effects of genetic variation on the function and antigenicity of the viral proteins at biosafety level 2. A few papers have reported pseudotyping RSV F and G on lentiviral particles (50–53), but those methods have not been widely used outside the papers themselves, and we were unable to generate appreciable infectious titers of F and G pseudotyped lentiviral particles by following the methods described in those studies (Fig. S1).

We initially focused on a lab-adapted, subtype A strain of RSV termed the "Long strain." To pseudotype RSV F and G on lentiviral particles, we transiently transfected 293T cells with expression constructs encoding codon-optimized F and G from the Long strain, lentivirus helper plasmids, and a lentivirus backbone plasmid encoding luciferase and ZsGreen (54) (Fig. 1A). Prior studies report that pseudovirus titers can be improved by truncating the cytoplasmic tails of the entry proteins from multiple virus families including paramyxoviruses (55–61). For RSV, we first evaluated tiled truncations of G's N-terminal cytoplasmic tail, which were each paired with full-length F. Titers measured on 293T target cells using a luciferase-based readout increased with longer truncations of the G cytoplasmic tail, and the highest titers were achieved with a 31-amino-acid deletion (Fig. 1B). We determined that the G cytoplasmic tail truncation increased the amount of both F and G protein expressed on pseudovirus particles as measured by Western blot (Fig. S2A and B), but did not impact the amount of pseudovirus particles produced as measured by p24 ELISA (Fig. S2C). We also tiled truncations of F's C-terminal cytoplasmic tail and paired these with the optimal G (31-residue cytoplasmic tail deletion). Titers were highest for conditions with the full-length F and shorter cytoplasmic tail truncations, but decreased with the deletion of 16 or more amino acids of the F cytoplasmic tail (Fig. 1C). Therefore, for all subsequent experiments in this paper, we used full-length F and G with a 31-amino-acid cytoplasmic tail deletion. Consistent with prior

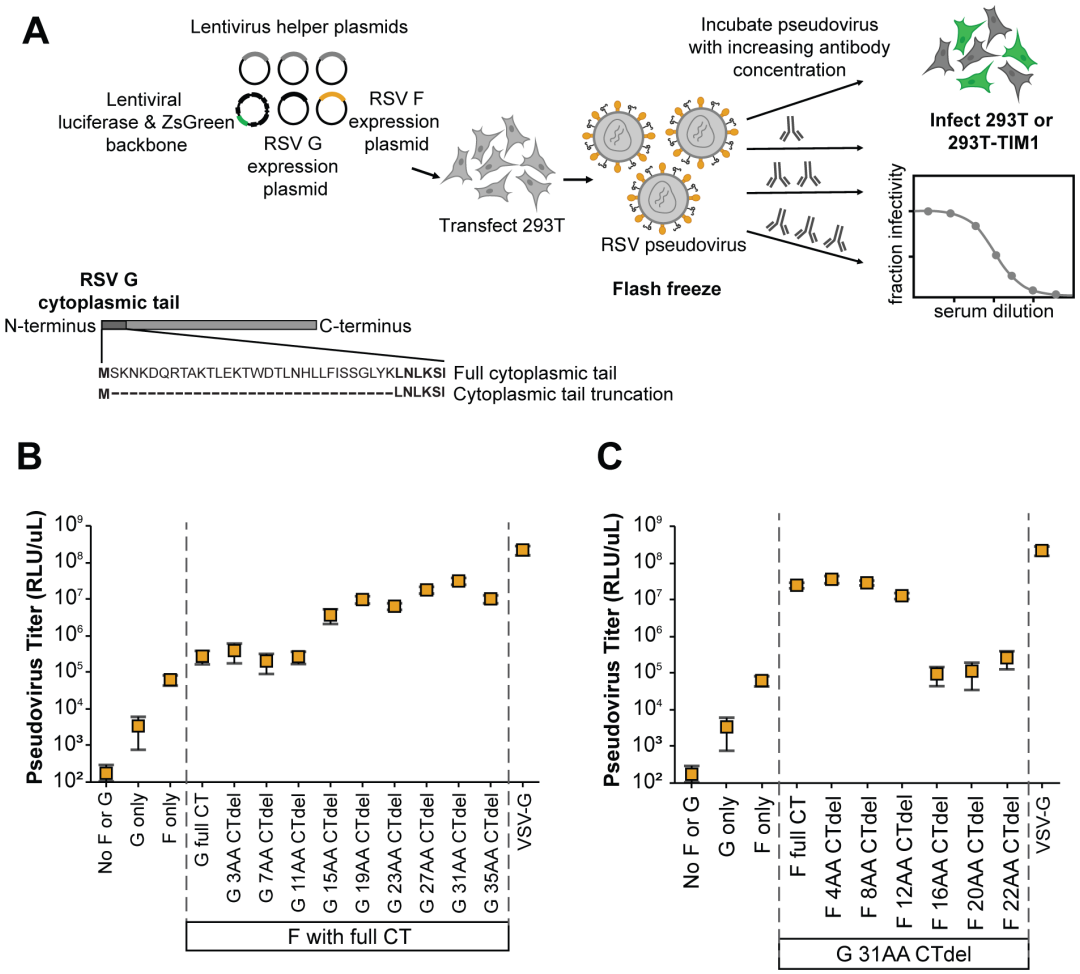

FIG 1 Generation of pseudoviruses with RSV F and G. (A) Process to create lentiviral particles pseudotyped with RSV F and G and then perform neutralization assays. To produce the pseudotyped particles, 293T cells are transfected with lentivirus helper plasmids (encoding Gag-Pol, Tat, and Rev) along with a lentiviral backbone plasmid (encoding luciferase and ZsGreen), and plasmids expressing codon-optimized F and G with a truncated N-terminal cytoplasmic tail (CT). Note G is a type II membrane protein, so the cytoplasmic tail is at the N-terminus. (B) Titers of pseudotyped lentiviral particles expressing the lab-adapted subtype A Long strain F and G increased when full-length F was paired with G with a N-terminal cytoplasmic tail truncation. The highest titers were achieved with a 31-amino-acid truncation of the tail; note that all subsequent experiments in this paper use G with this truncation. The plot shows particles pseudotyped with VSV-G as a positive control. Titers are reported in relative luciferase units per microliter (RLU/µL) following infection of 293T cells. Points indicate the mean ± standard error of two independent replicates. (C) Titers of pseudotyped lentiviral particles decreased with C-terminal cytoplasmic tail truncations of the F paired with the truncated G. Points indicate the mean ± standard error of two independent replicates.

studies of RSV, we found that flash freezing on dry ice and thawing at 37°C maintains pseudovirus infectivity (Fig. S3) (51, 62).

We next tested if we could produce high-titer pseudoviruses with F and G from other RSV strains in addition to the lab-adapted Long strain. We made pseudoviruses expressing codon-optimized F and G (with the 31-amino acid cytoplasmic tail deletion) from the subtype A lab-adapted A2 and subtype B lab-adapted B1 strains (Table S1). The pseudoviruses with F and G from these other two lab-adapted strains also yielded good titers of ~10^5 transducing units per milliliter on 293T cells (Fig. 2A).

Because F is the main target of monoclonal antibodies and vaccines (6), we next tested if we could produce pseudoviruses with F from clinical rather than lab-adapted RSV strains. We chose F proteins from direct sequencing of clinical specimens including subtype A strains from 1982 and 2020 and subtype B strains from 1982, 1992, 2019, and 2024 (Table S1). We paired the F proteins (expressed from codon-optimized gene sequences) from clinical strains with the truncated G from the lab-adapted subtype

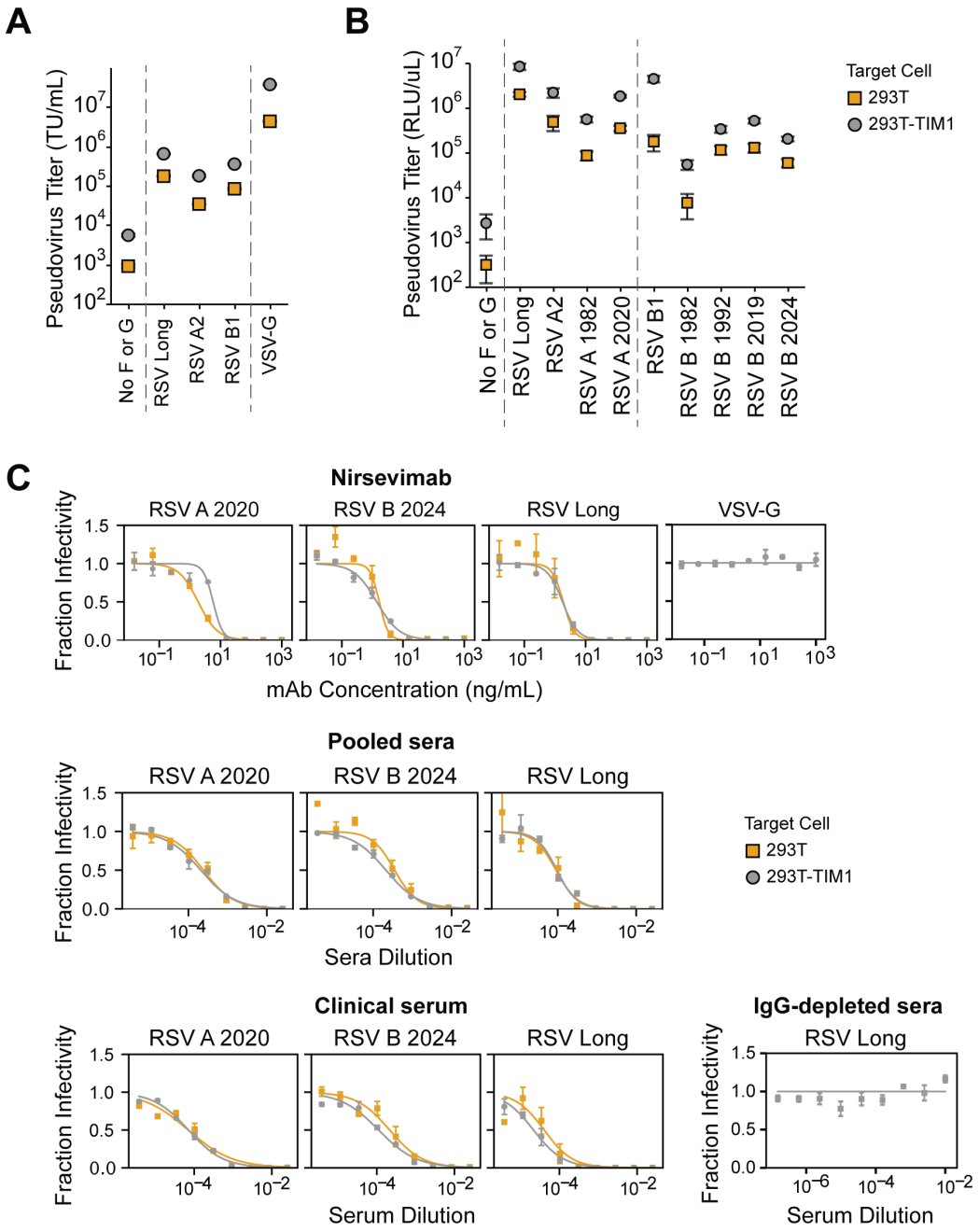

FIG 2 TIM1 expression increases infection of 293T cells by RSV pseudovirus without impacting neutralization. (A) Titers of RSV pseudoviruses are higher on 293T cells expressing TIM1 than unmodified 293T cells. Titers are shown for RSV pseudovirus expressing F and G from lab-adapted strains in transducing units per milliliter (TU/mL) using 293T or 293T-TIM1 target cells. VSV-G pseudotyped particles are shown as a positive control. Points indicate the mean ± standard error of two independent replicates. (B) F and G from a variety of subtypes A and B are lab-adapted, and clinical strains are efficiently pseudotyped on lentiviral particles. Titers in relative luciferase units per microliter (RLU/µL) measured on 293T or 293T-TIM1 cells for RSV pseudoviruses expressing F and G from lab-adapted strains (subtype A Long and A2, subtype B B1), or F from clinical sequences (A 1982, A 2020, B 1982, B 1992, B 2019, and B 2024) paired with Long G. Points indicate the mean ± standard error of two independent replicates. (C) Neutralization titers for RSV pseudoviruses are the same on 293T and 293T-TIM1 target cells. Neutralization curves for RSV pseudoviruses expressing F from clinical strains RSV A 2020 or B 2024 or from the lab-adapted Long strain paired with Long G against the F-directed monoclonal antibody Nirsevimab, recent pooled human sera, and a human serum specimen collected from a healthy adult in 1987. Pseudovirus expressing VSV-G is a negative control that is not expected to be neutralized by nirsevimab. IgG-depleted human sera from BEI resources were used as a negative control and tested for neutralization of RSV Long pseudovirus. Points indicate the mean ± standard error of technical replicates.

A Long strain and named the pseudoviruses based on the F protein (RSV A 1982, RSV A 2020, RSV B 1982, RSV B 1992, RSV B 2019, and RSV B 2024; Table S1). All of these pseudoviruses with clinical strain F proteins gave appreciable titers on 293T cells (Fig. 2B), although the titers were generally lower than for pseudoviruses with F from lab-adapted strains. Pseudoviruses expressing subtype A clinical strain F proteins generally produced higher titers compared to those with subtype B clinical strain F proteins (Fig. 2B). Pairing the F protein from clinical strains with the G protein from the Long strain yields similar to higher titers compared to pairing the F protein from clinical strains with the matched clinical strain G protein (Fig. S4A) and does not impact neutralization (Fig. S4B).

The titers of the RSV F and G pseudoviruses were further enhanced by infecting 293T target cells engineered to overexpress TIM1 (T-cell immunoglobulin and mucin domain 1, Fig. S5A), which can serve as a non-specific attachment factor for some viruses by binding to phosphatidylserine in the viral membrane (63). The pseudovirus titers were generally ~7-fold higher on 293T-TIM1 cells compared to unmodified 293T cells (Fig. 2A and B). Note that the inclusion of the G protein is less essential for good pseudovirus titers on 293T-TIM1 than 293T cells (Fig. S5B), but does still enhance titers on both cell lines. RSV pseudovirus titers were higher on 293T-TIM1 target cells than on A549, Hep2, or Huh7.5.1 cells (Fig. S5C and D).

We used pseudoviruses with F from three different RSV strains (the lab-adapted Long strain, and the clinical strains RSV A 2020 and RSV B 2024) paired with Long G to generate neutralization curves against the clinically relevant F-directed monoclonal antibody nirsevimab, a pool of recently collected human sera, and a serum sample collected from a healthy adult in 1987. All three RSV pseudoviruses were neutralized by the antibody and sera, and the neutralization was the same on 293T, 293T-TIM1, and A549 target cells (Fig. 2C; Fig. S5E). These data suggest that TIM1 expression does not affect the measured neutralization titers, so for all subsequent neutralization assays in this study, we used 293T-TIM1 target cells since they gave higher titers. We also found that the RSV pseudovirus must be diluted at least fourfold to make the neutralization titers independent of the pseudovirus dilution factor (Fig. S6A), possibly because undiluted transfection supernatant contains components that affect neutralization. Provided the pseudovirus was diluted at least fourfold, neutralization titers were otherwise similar across a range of input virus amounts (Fig. S6B).

Pseudovirus neutralization titers match expected values from a full-virus neutralization assay and for reference sera

We validated our neutralization assay with RSV pseudoviruses by comparing neutralization titers for 28 human serum specimens measured using our RSV A2 pseudovirus to recently published titers from an assay using full-length, replicative A2 virus (64). The titers measured with the pseudoviruses were nearly identical to those measured with the full-length virus (Fig. 3A; Fig. S7).

As further validation, we measured neutralization by three reference sera from BEI Resources against pseudoviruses with F and G from the A2 or B1 strains of RSV. The titers were highly reproducible across independent experiments performed on different days (Fig. 3B; Fig. S8A). To compare neutralization titers of the BEI Resources reference sera to published standardized neutralization titers, we also measured neutralization of the WHO International Standard Antiserum to RSV (NIBSC 16/284) against pseudoviruses with F and G from the A2 or B1 strains of RSV to calculate a conversion factor between pseudovirus neutralization titers and International Units per milliliter (IU/mL) (64–66) (Fig. S8A and B). These measurements were also highly reproducible across independent experiments (Fig. S8A). Standardized RSV pseudovirus neutralization assay titers for the BEI Resources reference sera against both A2 and B1 pseudoviruses were within 2-fold of the published reference values (Fig. 3C).

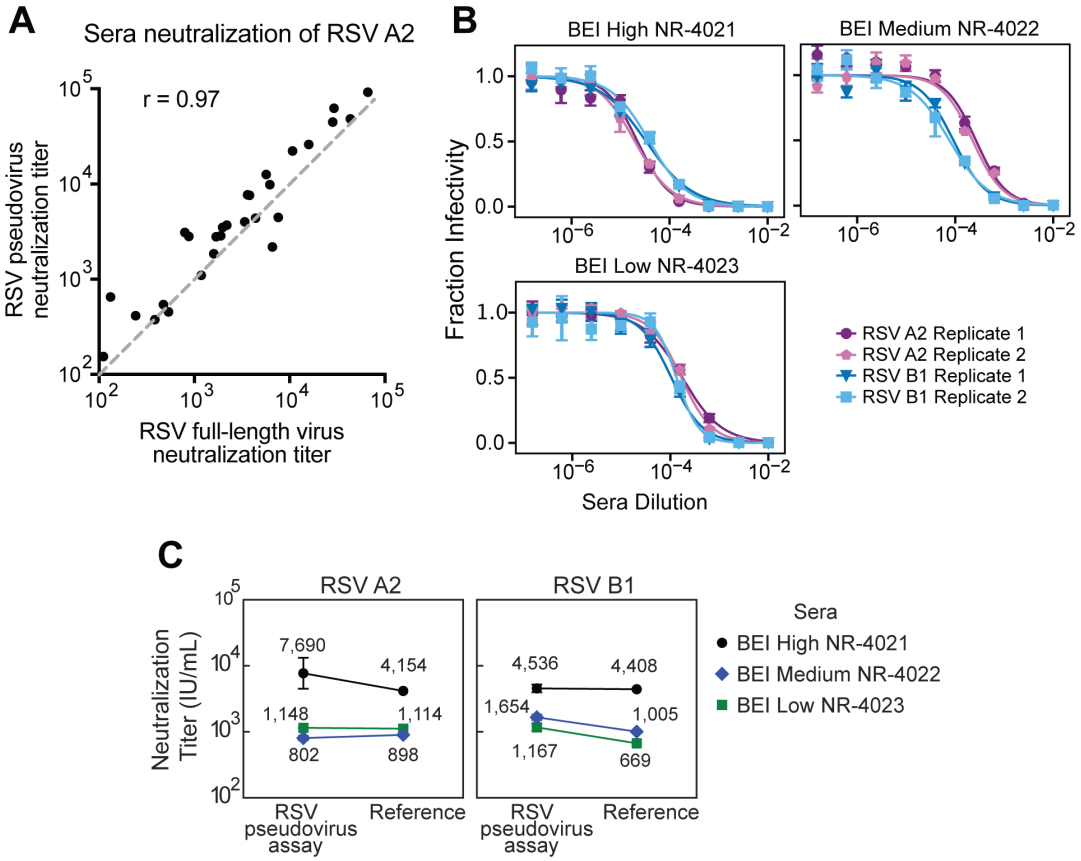

FIG 3 RSV pseudovirus neutralization titers match expected values from a full-virus neutralization assay and reference sera. (A) Correlation between neutralization titers against RSV A2 measured with our pseudovirus neutralization assay (*y*-axis) versus previously published values measured using full-length replicative RSV A2 (*x*-axis). 1:1 is shown by the gray dashed line. Neutralization titers are the reciprocal serum dilution at 50% fraction infectivity. Each point represents the geometric mean neutralization titer of two independent experiments for a different human serum sample. (B) Neutralization measurements are highly reproducible. Neutralization curves of pseudoviruses with F and G from the RSV A2 or B1 strains against three different reference sera from BEI Resources. Points indicate the mean ± standard error of technical repeats of experiments performed on the same day. Different replicates indicate independent experiments performed on different days. See Fig. S8 for additional independent replicates validating the reproducibility. (C) Neutralization titers for the three reference sera from BEI Resources match published values. Plots show neutralization titers for pseudoviruses expressing F and G from RSV A2 or B1 strains versus published neutralization values (64, 65). Neutralization titers were standardized to International Units per milliliter (IU/mL) as described in Fig. S8.

RSV pseudovirus neutralization assay measures F-directed neutralizing antibodies

Previously published RSV neutralization assays utilizing immortalized cell lines measure neutralization by F-directed but not G-directed antibodies. However, assays on primary cells or using complement on immortalized cell lines can measure G-directed neutralization (41, 67–70). To test the relative contributions of F- and G-directed antibodies to neutralization measured using our pseudovirus assay, we depleted a pool of recently collected human sera of G- or F-directed antibodies (Fig. 4A and B) and then measured neutralization of pseudoviruses with F and G from the Long strain (Fig. 4C). Depletion of F-directed antibodies dramatically decreased serum neutralization by over two orders of magnitude (Fig. 4C). In contrast, depletion of G-directed antibodies caused no appreciable change in neutralization. Therefore, the RSV pseudovirus neutralization assay measures serum neutralization that is almost entirely due to F-directed antibodies.

RSV F evolution does not erode polyclonal serum neutralizing titers

To determine if the evolution of RSV F erodes neutralization by human polyclonal serum antibodies, we measured neutralization of pseudoviruses with F from historical and

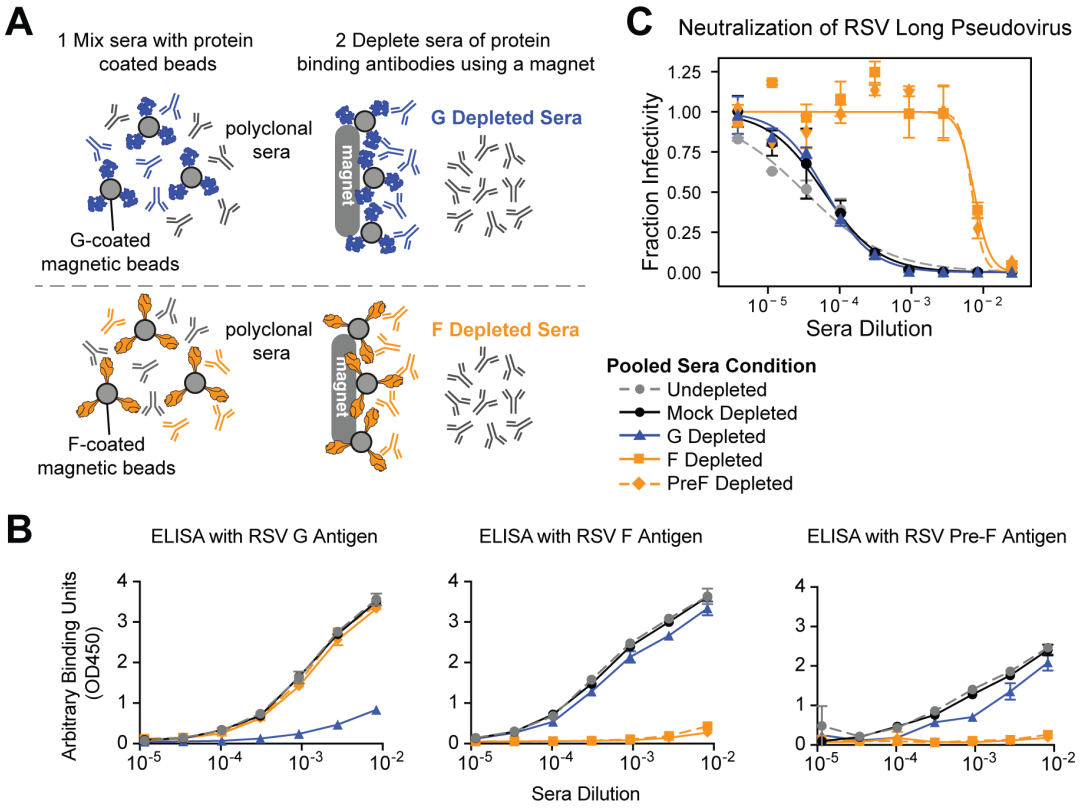

FIG 4 RSV pseudovirus neutralization assay measures F-directed neutralizing activity. (A) Process to deplete pooled polyclonal human sera of either G- or F-binding antibodies using G- or F-coated magnetic beads. Sera were depleted of G-directed antibodies using beads coated with the Long G protein and depleted of F-directed antibodies using beads coated with either unmodified or pre-fusion stabilized (PreF) Long F protein. (B) ELISA binding curves validate that the depletions nearly completely removed the G- or F-binding antibodies. The ELISA plates were coated with G, unmodified F, or pre-fusion stabilized F, all from the Long strain. Points indicate the mean ± standard error of two technical replicates. (C) Neutralization titers against pseudoviruses with the Long strain F and G decrease with depletion of F- but not G-directed antibodies. Shown is the neutralization of pseudovirus with Long F and G against sera depleted by the indicated method, or undepleted or mock-depleted sera. Points indicate the mean ± standard error of two technical replicates. All experiments shown in this figure utilized a pool of human sera collected in 2021.

recent RSV strains. Specifically, we used the F proteins from 1982 and 2020 strains of subtype A, or 1982, 1992, 2019, and 2024 strains of subtype B (Fig. 5; Table S1). The sequences for these proteins are all close to the trunk of the global RSV F phylogenetic trees rather than on long branches (Fig. 5), indicating that they are representative of strains from that time and do not have rare private mutations. The 1982 and 2020 subtype A proteins differ by only two amino-acid mutations, both in defined antigenic regions (71) (Fig. 5A). The 1982 and 2024 subtype B proteins differ by 10 amino acid mutations, 8 of which are in antigenic regions (Fig. 5B).

To test the effect of F's evolution on serum antibody neutralization, we used the approach in Fig. 6A. We assembled a panel of 20 historical sera collected from healthy adults between 1985 and 1987 (Table S2). No information was available about recent respiratory virus infections of these individuals, but since humans are regularly re-infected with RSV throughout adulthood (3, 72–74), most of these individuals were likely infected with a 1980s RSV strain within a few years preceding serum collection. None of the individuals would have been infected with recent strains prior to serum collection, since those strains did not yet exist. We depleted all sera of antibodies directed to G (from the Long strain) to ensure any measured neutralization was due to F-binding antibodies. We then measured neutralization by each historical serum of pseudoviruses with F from the historical and recent strains paired with G from the Long strain. If F evolution erodes serum antibody neutralization, then historical sera should neutralize

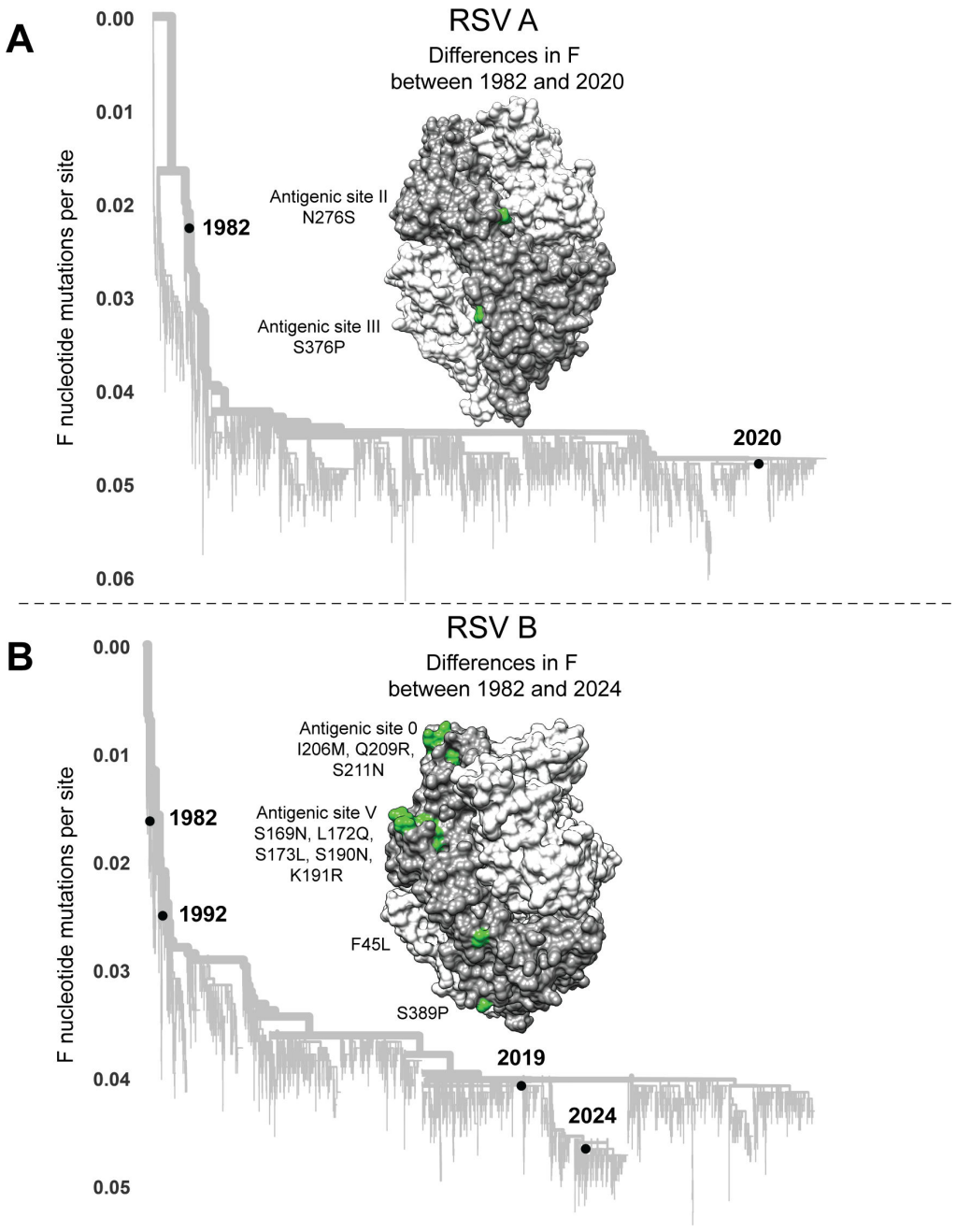

FIG 5 RSV strains used to study the effects of F evolution on serum and antibody neutralization. (A) Phylogenetic tree of subtype A RSV F gene sequences with black circles indicating the historical (1982) and recent (2020) sequences selected for study. Amino acid differences in F between the historical 1982 and recent 2020 sequences are shown in green on one protomer of the RSV F homotrimer (PDB 5C6B); the protomer with the amino acid differences indicated is in dark gray, and the other two protomers are in light gray. An interactive version of this phylogenetic tree can be found here: https://nextstrain.org/community/jbloomlab/RSV-evolution-neut@main/RSV-A-F. (B) Phylogenetic tree of subtype B RSV F gene sequences with black circles indicating the historical (1982 and 1992) and recent (2019 and 2024) sequences selected for study. Amino acid differences in F between the 1982 and 2024 sequences are shown on the F structure as in panel (A). An interactive version of this phylogenetic tree can be found here: https://nextstrain.org/community/jbloomlab/RSV-evolution-neut@main/RSV-B-F.

historical F strains better than recent F strains; otherwise, the strains should be similarly neutralized (see hypothetical data in Fig. 6A).

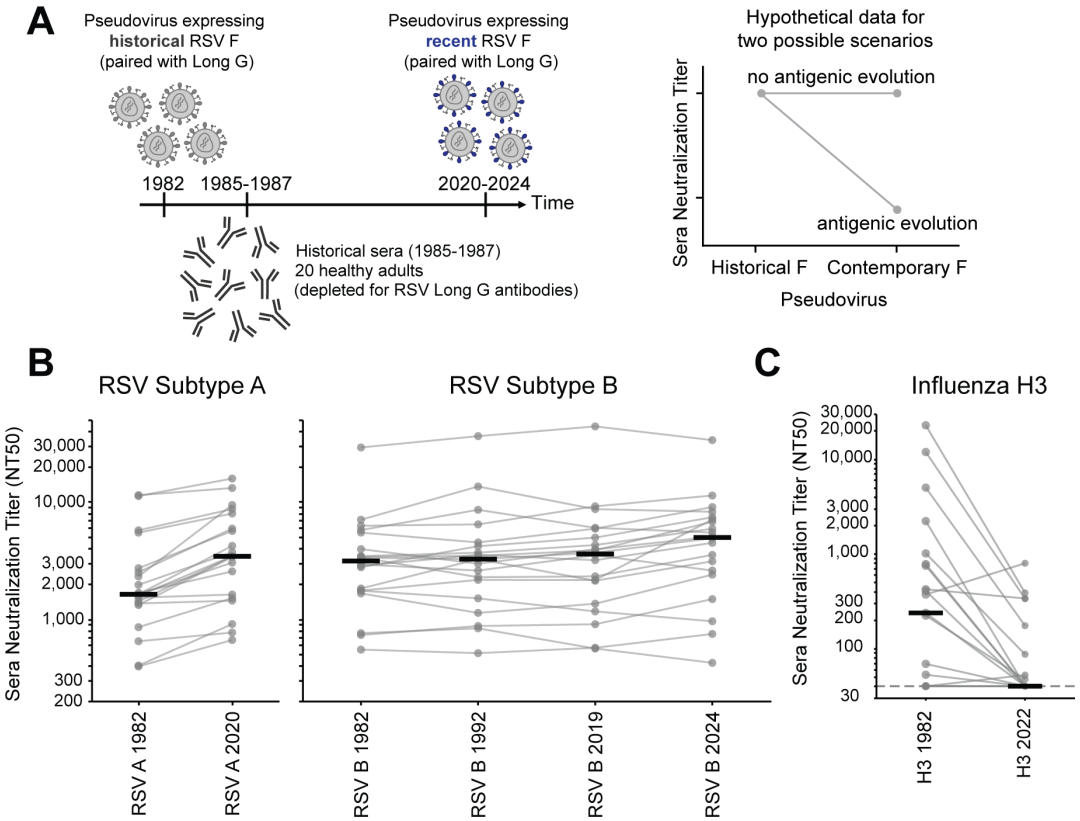

FIG 6 RSV F evolution does not strongly erode polyclonal serum antibody neutralization. (A) Design of experiment to test if F evolution erodes serum antibody neutralization. Historical sera collected from healthy adults in 1985-1987 were depleted for G-binding antibodies and then tested for neutralization of RSV pseudoviruses with G from the Long strain and F from either a historical (e.g., 1982) or a recent (e.g., 2020–2024) subtype A or B strain. The plot at right shows hypothetical data for two different scenarios: the sera are expected to neutralize pseudoviruses with the historical F (since it is from individuals who would have been infected with similar viruses), but will not neutralize pseudoviruses with the recent F if that protein undergoes rapid antigenic evolution. (B) Neutralization titers for 20 historical sera against the pseudoviruses expressing the Long strain G and F from historical and recent RSV A (left panel) or RSV B strains (right panel). Each set of gray dots connected by lines represents titers against a different serum (geometric mean of two independent experiments), and the black lines represent the median titer against that pseudovirus across all 20 sera. Individual neutralization curves are in Fig. S9. An interactive version of this plot colored by serum sample is available at https://github.com/jbloomlab/RSV-evolution-neut/blob/main/03_output/plots/RSVEvo_historicalsera_neutralization_plot_colored_interactive_subset.html. (C) Neutralization titers decrease for the same 20 historical sera against pseudoviruses expressing the hemagglutinin from an historical (A/Netherlands/233/1982) versus recent (A/Massachusetts/18/2022) strain of human H3N2 influenza. Dots and lines have the same meaning as in panel (B). Individual neutralization curves are in Fig. S10.

Neutralization by historical sera was similar for pseudoviruses expressing historical and recent F proteins from both RSV subtypes A and B (Fig. 6B; Fig. S9). Specifically, most individual sera neutralized pseudoviruses with F proteins of the 1982 and 2020 subtype A strains at similar titers, and likewise for pseudoviruses with the F proteins of subtype B from 1982, 1992, 2019, and 2024 strains (Fig. 6B). This lack of erosion of serum neutralization by RSV F evolution contrasts with similar experiments with the same sera against pseudoviruses with influenza hemagglutinin from historical versus recent human H3N2 strains, which show that influenza hemagglutinin evolution largely escapes serum neutralization over the same timeframe (Fig. 6C; Fig. S10). We note that prior experiments on other sera have also shown rapid erosion of neutralization by the evolution of the spikes of CoV-229E and SARS-CoV-2 (75, 76). Overall, these results suggest that RSV F evolution does not rapidly erode polyclonal serum antibody neutralization, in contrast to the evolution of influenza hemagglutinin and spike proteins of SARS-CoV-2 and CoV-229E.

Natural evolution of RSV F escapes some monoclonal antibodies

Even if RSV F's evolution does not strongly erode neutralization by polyclonal serum antibodies, it could lead to escape from individual monoclonal antibodies. Indeed, sporadic RSV strains have been reported to carry mutations that escape nirsevimab, which is clinically used for RSV prevention for infants (32, 35–37). These known escape mutations (K68Q/N and N201S/T) are found in a few sequences scattered across the global RSV-B F phylogenetic tree (Fig. 7A). We chose F proteins from recent RSV B strains with the K68Q, N201S, and N201T nirsevimab escape mutations to test for neutralization by monoclonal antibodies, also testing the more representative historical and recent RSV F proteins described in the previous section.

Pseudoviruses expressing the representative F proteins from both recent and historical RSV A and B strains were all neutralized by nirsevimab as well as four other monoclonal antibodies that are in clinical use (palivizumab [77, 78]), clinical trials (clesrovimab [79]) or pre-clinical studies (AM14 [80] and MPE8 [81]) (Fig. 7A; Fig. S11). However, two other antibodies (suptavumab [34] and hRSV90 [82]) failed to neutralize the representative recent RSV B strain (Fig. 7A; Fig. S11). We note that the failure of suptavumab to neutralize recent RSV B strains was already known, but was discovered only through the costly failure of a phase III clinical trial of this antibody in humans (34).

Pseudoviruses expressing F from recent RSV B strains with the K68Q, N201S, or N201T mutations were strongly resistant to nirsevimab and also escaped suptavumab and hRSV90 (Fig. 7A; Fig. S11). These results highlight the potential for recent RSV B F variants to evolve to escape neutralization by a monoclonal antibody in clinical use and emphasize the importance of using assays like the one we describe here to monitor for resistance in recent strains.

We next evaluated whether the recent F proteins with the sporadic mutations that escape nirsevimab also have reduced neutralization by polyclonal human sera. To do this, we tested the neutralization of the pseudoviruses expressing recent RSV B F proteins with the N201S/T mutations against the 20 historical sera described in the prior section (again depleted of G antibodies). A number of the sera showed modestly reduced neutralization of F with the N201S/T mutations relative to the F of representative recent RSV B strains that lack these mutations (Fig. 7C; Fig. S12). Therefore, for some sera, a measurable fraction of the neutralization is due to antibodies targeting an epitope similar to that bound by nirsevimab, and so nirsevimab resistance mutations can also influence serum neutralization.

DISCUSSION

We developed a pseudotyping system to quantify how evolution of RSV F affects antibody neutralization. We found that efficient pseudotyping of RSV F and G on lentiviral particles requires truncation of the G cytoplasmic tail, and that titers were further improved by the use of TIM1-expressing target cells. With this system, we produce high titers of pseudovirus expressing F from clinical strains of both RSV subtypes A and B. Neutralization titers measured using these pseudoviruses closely match those from a full-length replicative virus assay.

We found that the evolution of F, even over several decades, only modestly affects neutralization by human polyclonal serum antibodies. Therefore, RSV F stands in clear contrast to the entry proteins of human seasonal influenza and coronaviruses, which evolve to rapidly erode serum antibody neutralization (26, 75, 76). Further work will be needed to determine why RSV F has a slower rate of antigenic change than some other viral entry proteins, but possible hypotheses are that F is less tolerant of mutations (83, 84) or that polyclonal serum antibodies target so many distinct F epitopes that individual mutations are unable to provide much antigenic benefit to the virus (85). Despite the lack of strong erosion of F-directed neutralization by RSV evolution, humans are reinfected by RSV multiple times throughout their lives (2, 3, 74, 86). The fact that these reinfections occur despite F's relatively slow antigenic evolution suggests that either

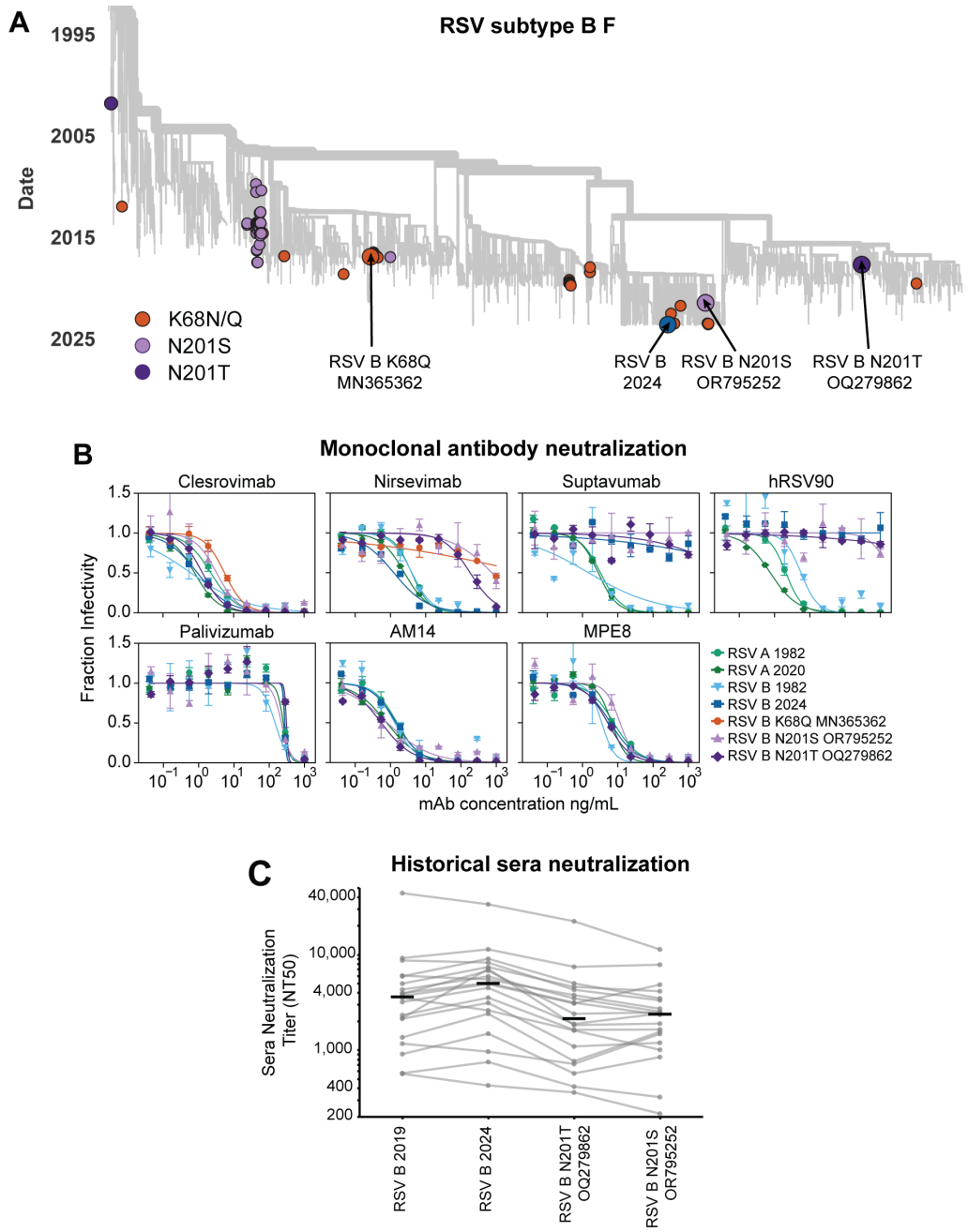

FIG 7 Natural evolution of RSV F escapes some monoclonal antibodies. (A) Phylogenetic tree of F gene sequences from recent subtype B RSV strains, with colored circles indicating the representative RSV B 2024 strain used in our experiments as well as other strains containing known nirsevimab resistance mutations. Arrows indicate F proteins used in our experiments. (B) Neutralization curves for monoclonal antibodies versus pseudoviruses expressing the indicated F protein paired with Long G. Points indicate the mean ± standard error of technical replicates. Neutralization curves for these monoclonal antibodies from a separate experiment performed on a different day as well as versus pseudoviruses expressing F and G from lab-adapted strains are in Fig. S11. (C) Neutralization titers for the 20 historical sera against pseudoviruses expressing the indicated F protein paired with Long G. Each set of gray dots connected by lines represents titers against a different serum (geometric mean of two independent experiments), and the black lines represent the median titer against that pseudovirus across all 20 sera. The historical sera are the same as those used in Fig. 6B and C and are depleted of antibodies that bind to Long G. The points for the RSV B 2019 and RSV B 2024 strains shown in this panel are the same as those shown in Fig. 6B. See Fig. S9 and S12 for the neutralization curves.

F-directed neutralizing antibody titers wane over time (87–90), or that F-directed neutralizing antibodies are not actually as protective as widely believed—although this second explanation would seem at odds with studies indicating good efficacy of anti-F vaccines and monoclonal antibodies in humans (6–17). In either case, the fact that reinfections can occur even without much F antigenic evolution could in turn lead to less immune pressure on F to evolve antigenically.

However, our results confirm that the natural evolution of F does result in escape from some individual monoclonal antibodies. In particular, we confirmed that more recent subtype B strains have escaped monoclonal antibodies (e.g., suptavumab and hRSV90) that target a prefusion-specific antigenic region near the trimer apex, consistent with prior studies (34, 91).

The fact that monoclonal antibody nirsevimab is now being widely administered to infants in the United States and some other countries could increase the evolutionary pressure on F (20, 92). We confirmed that rare RSV B strains have sporadic mutations that confer escape from nirsevimab (32, 35–37). Nirsevimab targets an epitope on the apex of the F trimer that is relatively close to the region targeted by the antibodies suptavumab and hRSV90 that are now escaped by most recent subtype B strains (34, 82, 93). Therefore, it may be advisable to consider cocktails with additional antibodies targeting other RSV epitopes. We also note that the antibody escape mutations observed to date seem to be mostly in RSV B (32, 34–37), which has accumulated more mutations than RSV A over the last few decades.

We found that the currently rare nirsevimab escape mutations in some RSV B strains also measurably reduced F-directed neutralization by the polyclonal antibodies in some sera. This finding suggests that an appreciable fraction of neutralization by some sera is due to antibodies targeting the apex of the F trimer near the nirsevimab site (8, 71). Therefore, as nirsevimab (and possibly future monoclonal antibodies) are more widely administered, it will be important to monitor not only for resistance to the antibodies themselves, but also evaluate if any resistance mutations affect neutralization by polyclonal antibodies elicited by infection or vaccination. The pseudovirus assay we describe here will therefore be a valuable tool to continue to monitor how new antibodies and vaccines affect and are affected by RSV evolution.

Limitations of study

Our RSV pseudovirus neutralization assay measures only F-directed neutralizing antibodies. The G protein is maintained by RSV in nature, so it is clearly important for viral infection of airway cells during human infections, but is largely dispensable for viral infection of immortalized cell lines (52, 53, 94, 95). G is particularly dispensable on the 293T-TIM1 cells used in our paper, likely because TIM1 binding to phosphatidylserine on the virion can mediate attachment (63). Note that most other established RSV neutralization assays also only measure F-directed neutralization (8, 67–70, 94). Despite the inability of our assay to measure G-directed neutralization, G is under stronger pressure for adaptive evolution than F during actual RSV evolution (30), suggesting G-directed antibodies play an important role in human immunity. The use of TIM1-overexpressing cells may interfere with future applicability to study G, since TIM1 promotes viral attachment in the same way that G is thought to promote attachment in actual primary airway cells. Our pseudovirus assay also does not measure other immune mechanisms that could be relevant to RSV immunity, including T-cells and antibody effector functions.

Additionally, the pseudotyped lentiviral particles used in our assays likely have a different morphology and density of F and G glycoproteins than authentic RSV, which could influence some aspects of antibody neutralization. We also note that the nucleolin protein thought to act as a co-receptor for F may be more highly expressed in cell lines like the ones used for our assay than in primary human airway cells (96, 97).

The fact that our pseudoviruses are based on lentiviral particles also precludes their use on serum samples from people living with HIV who are being treated with antiretro-

virals, since these antivirals will interfere with reverse transcription or integration of the lentiviral genome.

Our experiments primarily used sera collected in the 1980s from healthy adults, but no information is available about recent respiratory virus infections of these individuals. It is possible that the titers and specificities of serum antibodies could differ in individuals of other ages or exposure histories.

MATERIALS AND METHODS

Serum samples

The following reagent was obtained through BEI Resources, NIAID, NIH: Panel of Human Antiserum and Immune Globulin to Respiratory Syncytial Virus, NR-32832. The WHO First International Standard Antiserum to Respiratory Syncytial Virus 16/284 was obtained from NIBSC, product number 16/284. See Table S2 for available metadata on historical serum samples used in this study and the recently published study by Piliper et al. (64) for sera used for pseudovirus assay validation. Pooled human sera collected in 2021 were purchased from the Program in Immunology at the Fred Hutch Cancer Center. All sera were heat inactivated at 56°C for 1 h and then stored long term at −80°C. For assays assessing serum neutralization of influenza HA and NA expressing pseudovirus, sera were treated with receptor destroying enzyme as described previously (98).

Antibodies

The RSV monoclonal antibodies palivizumab (78), nirsevimab (22), suptavumab (34), clesrovimab (99), and hRSV90 (82) were produced by Genscript as human IgG1 kappa isotypes. AM14 (80) and MPE8 (81) were kindly provided by Neil King at the University of Washington. The sequences for heavy and light chains are at https://github.com/jbloomlab/RSV-evolution-neut/blob/main/03_output/summary_tables/RSV_mAb_AAseq.csv. Sequences were obtained from the referenced publications, structures in the Protein Data Bank or original patents. hRSV90 amino acid sequence was obtained from the Protein Data Bank (PDB) 5TPN. Palivizumab originated from patent US6955717B2.

Cell line handling

All cell lines were cultured in D10 media (Dulbecco's modified Eagle medium supplemented with 10% heat-inactivated fetal bovine serum, 2 mM L-glutamine, 100 U/mL penicillin, and 100 mg/mL streptomycin) and cultured at 37°C with 5% CO_2.

Creation and validation of the 293T-TIM1 cells

Human TIM1 (GenBank: AAC39862.1) followed by 2A peptide and mTagBFP2 was cloned into the pHAGE2 lentivirus vector. TIM1 lentivirus pseudotyped with VSV-G was rescued from 293T cells and used to transduce 293T cells. Note that low titers of this virus were obtained probably due to TIM1 binding virions to producer cells, but we did obtain sufficient titers for transduction. After picking and expanding a single 293T clone, immunostaining was performed to confirm the expression of TIM1 (see Fig. S5A). For this immunostaining, 293T and 293T-TIM1 cells were digested by trypsin and resuspended into single cells with 1% BSA. The cells were stained with anti-TIM1 primary antibody (AF1750-SP, R&D Systems) diluted in 1% BSA at 1:100 for 1 h on ice. After three washes with PBS, the cells were stained with 488-conjugated donkey anti-goat IgG secondary antibody (A-11055, ThermoFisher) diluted in 1% BSA at 1:1,000 for 1 h on ice. After three washes with PBS, the cells were resuspended in 1% BSA for flow cytometry analysis.

Phylogenetic analysis of RSV F

NextStrain RSV phylogenetic trees are maintained and available at nextstrain.org/rsv (100). These trees display a subsample of available sequences and are updated over time. To visualize all available sequences at the time of our analysis without subsampling, we utilized the workflow at https://github.com/nextstrain/rsv and removed the subsampling steps to construct subtypes A and B F trees containing all sequences as on 9 May 2024 (Fig. 5). Interactive versions of these trees are available at https://nextstrain.org/community/jbloomlab/RSV-evolution-neut@main/RSV-A-F and https://nextstrain.org/community/jbloomlab/RSV-evolution-neut@main/RSV-B-F.

Plasmids encoding viral entry proteins

The RSV F and G's used in experiments as well as the influenza HA and NA's are detailed in Table S1 including accession numbers. For RSV G's, we deleted 31 amino acids from the N-terminal cytoplasmic tail as shown in Fig. 1. RSV Long F and G codon-optimized sequences were obtained from a previously published study (52, 53). All other RSV F and G sequences were human codon optimized using a tool by GenScript found at https://www.genscript.com/tools/gensmart-codon-optimization. Codon-optimized sequences were then modified to remove homopolymers (>5 nucleotides) and premature poly A signals (AATAAA), which have previously been shown to impact RSV F protein synthesis from transfection (101, 102).

The A/Netherlands/233/1982 (H3N2) HA, A/Massachusetts/18/2022 (H3N2) HA, and A/Massachusetts/18/2022 (H3N2) NA sequences were human codon optimized by GenScript. The A/HongKong/1/1968 (H3N2) NA sequence was human codon optimized by Twist. No further modifications were made to these codon-optimized sequences.

We then had the genes synthesized commercially and cloned them into an HDM/CMV driven expression plasmid 27_HDM-tat1b after cutting with NotI and HindIII with the NEBuilder Hifi DNA Assembly Kit, incubating at 50°C for 30 min to 1 h, and transformed into Stellar competent cells (Takara, Cat. #636763) or NEB 5-alpha Competent *Escherichia coli* (NEB, Cat. #C2987H). All plasmids were confirmed by whole plasmid sequencing by Plasmidsaurus. The resulting plasmids are linked in Table S1 and the full plasmid maps are at https://github.com/jbloomlab/RSV-evolution-neut/tree/main/04_plasmid_maps. Relevant expression plasmids for the RSV F and G sequences can also be found on AddGene at https://www.addgene.org/browse/article/28253256/ (HDM_RSV_B1_F product ID 237353, HDM_RSV_B1_G_31AACTdel product ID 237354, HDM_RSV_A_1982_F product ID 237355, HDM_RSV_A_2020_F product ID 237356, HDM_RSV_B_1982_F product ID 237357, HDM_RSV_B_1992_F product ID 237358, HDM_RSV_B_2019_F product ID 237359, HDM_RSV_B_2024_F product ID 237360, HDM_RSV_B_MN365362_F_K68Q product ID 237361, HDM_RSV_B_OQ279862_F_N201T product ID 237362, and HDM_RSV_B_OR795252_F_201S product ID 237363).

We generated N-terminal cytoplasmic tail deletions to G by PCR amplification from the full-length RSV Long G using primers to delete the desired number of amino acids. C-terminal cytoplasmic tail deletions to F were generated by PCR amplification from the full-length RSV Long using primers to introduce a stop codon. These gene fragments were cloned into the expression vector as described above.

All plasmid maps are available at https://github.com/jbloomlab/RSV-evolution-neut/tree/main/04_plasmid_maps. The lentivirus helper plasmids are available from AddGene: HDM-tat1b product ID 204154, pRC-CMV-Rev1b product ID 20413, HDM-Hgpm2 product ID 204152 (103). The VSV-G expression plasmid used as a positive control is also available from AddGene: HDM_VSV_G product ID 204156. A lentiviral backbone plasmid that uses a CMV promoter to express luciferase followed by an IRES and ZsGreen is available from AddGene pHAGE-CMV-Luc2-IRES-ZsGreen-W product ID 164432 (54).

Generation and titration of pseudotyped lentiviral particles encoding luciferase and ZsGreen

We generated pseudovirus expressing RSV F and G and encoding luciferase and ZsGreen as shown in Fig. 1. To make RSV pseudovirus, 293T cells were plated the day before transfection in D10 to achieve ~70% confluency on the day of transfection. The cells were plated in either six-well dishes (600,000 cells per well), 10 cm dishes (4,000,000 cells) or 15 cm dishes (11,000,000 cells) depending on the desired volume of viral supernatant. Sixteen to twenty-four hours after plating, 293Ts were transfected using BioT (Bioland Scientific) with the appropriate µg of plasmid DNA designated in the product manual. For example, in a single well of a six-well dish, 2 µg total of DNA was transfected split up between 1 µg of the lentiviral backbone plasmid encoding luciferase and ZsGreen, 200 ng of RSV F expression plasmid, 100 ng RSV G expression plasmid, and 233 ng each of lentiviral helper expression plasmids 26_HDM-Hgpm2 (Gagpol), 27_HDM-tat1b (Tat), and 28_pRC-CMV-Rev1b (Rev). If producing in larger plates, DNA was scaled up accordingly, keeping the proportions the same between plasmids. After around 48 h the supernatant was filtered using a 0.45 µm syringe filter. Aliquots of viral stocks were then labeled and flash-frozen using a prechilled CoolRack CF45 Cooling Block (Fisher Cat. #UX-04392-51) on dry ice until frozen solid (around 15 min) before transferring to −80°C for long-term storage.

To titrate these pseudoviruses (Fig. 1 and 2), we seeded 60,000 target cells (293T or 293T-TIM1 cells) per well in 100 µl D10 on 96-well plates the day before infection to achieve 90% confluency at infection. We plated in white-walled, clear bottom 96-well plates for luciferase measurements and clear 96-well plates for ZsGreen measurement by flow cytometry. Sixteen to twenty-four hours after plating, aliquots of RSV pseudovirus were thawed in a 37°C water bath and serially diluted in 96-well plates. Technical replicates were performed within each experiment. We then added 100 µL of diluted virus per well to the cells for infections. If determining viral titer by flow cytometry, prior to transferring virus dilutions, two to four wells of the 96-well plate were trypsinized and counted to determine cell count per well at the time of infection for TU/mL calculations. Titer plates were harvested at 48–72 h following infection.

If determining titers by luciferase, we measured RLU using the Bright-Glo Luciferase Assay System (Promega, Ref. No. E2620). Briefly, 150 µL of media was aspirated from wells to leave ~30 µL per well before adding 30 µL of BrightGlo reagent per well to each well of the white 96-well plate for a 1:1 vol ratio in each well. To reduce background luminescence, we placed a white sticker to mask the clear bottoms of all wells or transferred to opaque white plates. We measured luminescence activity with a plate reader. For readings that were in the linear range, we normalized counts to volume to generate RLU/µL. For each pseudovirus, we calculated an RLU/µL from technical replicates by taking the mean of all individual replicates.

If determining titers using flow cytometry based on percent positive ZsGreen cells, wells with ~1–10% green cells were estimated by eye, trypsinized from the plate, spun down in a V-bottom 96-well plate, and washed three times with 1–3% BSA in PBS. Washed cells were then read on a flow cytometer, and the percentage of ZsGreen positive cells was determined based on gating of uninfected wells in FlowJo. This, along with the cell count per well on the day of infection, was used to calculate TU/mL (transducing units per mL).

We generated pseudovirus expressing influenza HA and NA using a similar protocol as described above with a few modifications. 293T cells were plated in 10 cm dishes the day before transfection in D10 to achieve ~70% confluency on the day of transfection. Sixteen to twenty-four hours after plating, 293Ts were transfected using BioT (Bioland Scientific) with 11.25 µg of DNA total per dish, 5 µg of lentiviral backbone encoding luciferase and ZsGreen, 1.25 µg each of lentiviral helper plasmids, 1.25 µg HA, 0.25 µg NA, and 1 µg of the HAT protease that activates HA. Twelve to sixteen hours post-transfection, media was swapped from D10 to IGM (influenza growth media) (98). Viral supernatant was collected around 48 h post-transfection by syringe filtering through

a 0.45 µm filter. Aliquots were stored at −80°C. To determine viral titers by luciferase, MDCK-SIAT1 cells (104) were plated on the day of infection around 2 h before infection by adding 15,000 cells per well in 50 µL of NAM (neutralization assay media, consisting of Medium-199 supplemented with 0.01% heat-inactivated FBS, 0.3% BSA, 100 U/mL penicillin, 100 µg/mL streptomycin, 100 µg/mL calcium chloride, and 25 mM HEPES) (105) supplemented with 2.5 µg/mL Amphotericin B, which increases pseudovirus titers (103). Serial dilutions of pseudovirus were then set up in NAM supplemented with 500 nM of oseltamivir, which inhibits neuraminidase from cleaving sialic acids on target cells, therefore making entry more efficient. The dilution plate was incubated on ice for 20 min for oseltamivir to bind. Then, 100 µL of each serial dilution was added to previously plated cells. After adding pseudovirus, the MDCK-SIAT1 plate was incubated for 48 h. To read titer for luciferase activity, BrightGlo was added, and plates were read as described above for RSV.

RSV F- and G-binding antibody depletion from sera and validation of depletion

We depleted sera of F- or G-binding antibodies as shown in Fig. 4. We obtained commercially available His-tagged, soluble RSV G protein based on the Long strain from SinoBiological (Cat: 40041-V08H). Soluble RSV F protein based on the Long strain, both unmodified and stabilized in the pre-fusion conformation using the SC-DM mutations as previously described (106), was produced by the removal of the transmembrane and cytoplasmic tail domains and addition of a trimerization domain (107) and N-terminal His-tag. The proteins were produced with pCMV/R vectors using endotoxin-free DNA in ExpiHEK293F cells grown in suspension using Expi293F expression medium (Life Technologies) at 33°C, 70% humidity, 8% CO_2 rotating at 150 rpm. The cultures were transfected using PEI-MAX (Polyscience) with cells grown to a density of 3.0 million cells per mL and cultivated for 3 days. Supernatants were clarified by centrifugation (5 min at 4,000 rcf), addition of PDADMAC solution to a final concentration of 0.0375% (Sigma Aldrich, #409014), and a second centrifugation (5 min at 4,000 rcf). The secreted proteins were purified from cell supernatant by IMAC, followed by SEC on a Superdex 200 10/300 Gl (GE Healthcare) equilibrated in 50 mM Tris pH 7.4, 250 mM NaCl, 50 mM Glycine, and 5% vol/vol Glycerol.

Magnetic Dynabeads for His-tag isolation and pulldown (Invitrogen Cat. #10104D) were aliquoted (100 ul per condition) and washed once with PBS in a magnetic stand. After the removal of supernatant, washed beads were resuspended in 10 µg protein (or PBS for mock conditions). Beads were incubated with protein for 10 min at 4°C on a rocker to allow his tagged protein to bind with the magnetic beads. After incubation, the beads were washed two times, and the supernatant was discarded. Beads were then resuspended in 100 µL sera. Serum and bead mixture was incubated on a rocker at 4°C overnight. After overnight incubation, samples were placed on a magnetic rack for 2 mins to separate antibodies bound to protein-conjugated beads from supernatant. The supernatant was collected, and a second round of depletion was performed. Depleted sera were stored at −80°C.

We validated depletion of RSV F- or G-binding antibodies from sera by ELISA (Fig. 4B). Immunlon 2HB 96-well plates (Thermo Scientific 3455) were coated with 100 µL of RSV Long F, preF or G protein at 1 µg/mL for 30 min at 37°C in PBS. Unbound protein was then removed by washing three times in PBS + 0.1% Tween-20 (PBS-T). Plates were blocked for 1 h at room temperature in 200 µL per well 5% (wt/vol) dried milk in PBS-T. Blocking buffer was removed, and sera/mAbs from serially diluted sera were added (100 µL per well) and incubated at 37°C for 1 h. After incubation, plates were washed three times in PBS-T and then incubated for 1 h at 37°C in secondary antibody HRP-conjugated goat anti-human IgG (Bethyl Labs, Cat. #A80-104P) at a dilution of 1:2,000 in blocking buffer (50 µL per well). Secondary antibody was washed off with three washes in PBS-T. Plates were developed with 100 µL TMBE for 4 min and stopped with 100 µL 1 N HCL before reading absorbance (450 nm) on a plate reader.

Pseudovirus neutralization assays

Neutralization assays with pseudovirus were performed as previously described with the modifications described below (54, 75). To perform neutralization assays using pseudoviruses expressing RSV F and G, we plated 293T-TIM1 cells (60,000 per well) in 96-well white-walled clear-bottom tissue culture treated plates 16–24 h prior to setting up the neutralization assay. Serum samples were diluted 1:10 or 1:50 in D10 and then serially diluted 3-fold for a total of nine dilutions per serum. Monoclonal antibodies were diluted to 1,000 ng/mL with nine total 3- or 3.5-fold serial dilutions. 50 µL of these diluted serum or mAb samples was then added to 96-well "set-up" plates in duplicate (two columns) per serum sample. Pseudoviruses expressing RSV F and G were then diluted the appropriate amount to achieve 600,000 to 2,000,000 RLU per well. These dilution factors varied per virus due to differences in titer (Fig. 1A and B) but were always diluted at least twofold (Fig. S6). 50 µL of diluted virus was then added to assay "set-up" plates that contain 50 µL of serum or mAb (note that pseudovirus is therefore diluted at least fourfold after this step, Fig. S6) as well as 50 µL of virus only added to 50 µL of D10 as a virus only control, and "set-up" plates were incubated for 1 h at 37°C with 5% CO_2. After the incubation, 100 µL per well of the set-up plate was transferred to the plated target cells. These plates were then incubated for 48 h before reading the luciferase signal as described above for pseudovirus titration.

Neutralization assays for pseudoviruses expressing influenza HA and NA were performed similarly to those using RSV pseudoviruses with a few differences. As described for titration of viruses, MDCK-SIAT1 cells were plated in clear-bottom white-walled 96-well tissue culture plates 2 h before infection. The cells were plated in 50 µL of NAM supplemented with amphotericin B. Serum samples were first treated with RDE, which resulted in a 1:4 dilution of sera. This initial dilution was accounted for when setting up serially diluted sera with a starting dilution of 1:10. Serum dilutions and virus dilutions were done in NAM, and virus dilutions were supplemented with 500 nM of oseltamivir. The rest of the assay was performed as described above for RSV pseudotyped lentivirus.

Fraction infectivity was calculated as compared to a no-serum or no-antibody well. Neutralization curves were then fit to the data using the neutcurve package (https://jbloomlab.github.io/neutcurve/) (108).

p24 ELISA

Lentiviral particle p24 protein concentration in RSV pseudovirus preparations was quantified using the QuickTiter Lentivirus-Associated p24 ELISA Kit (Cell Biolabs, Inc.) following the manufacturer's instructions. Briefly, viral supernatants were diluted in assay diluent. Samples were added to a 96-well plate pre-coated with an anti-p24 monoclonal antibody and incubated according to the kit protocol. Bound p24 was detected with an HRP-conjugated secondary antibody and visualized using TMB substrate. Absorbance was measured at 450 nm, and p24 concentrations were calculated from a standard curve generated with recombinant p24 protein provided in the kit. Lentiviral particle concentrations were estimated using the conversion provided in the kit manual, assuming that 1 ng of p24 corresponds to approximately 1.25×10^7 lentiviral particles. Values are reported as lentiviral particles per mL (Fig. S2C).

SDS-PAGE and western blotting

RSV Long pseudovirus expressing Long F paired with either G with a 31-amino-acid cytoplasmic tail truncation or full cytoplasmic tail was produced as described above and concentrated using ultracentrifugation with a 20% sucrose cushion at 100,000 g for 1 h. The pseudoviruses pelleted to the bottom of the cushion, and the pellets at the bottom of the tube were resuspended in PBS. Soluble RSV G, native F, and stabilized PreF proteins, along with RSV pseudovirus preparations, were prepared for SDS-PAGE by mixing with Sample Loading Buffer for Western Blots (LI-COR, Cat. No. 928-40004) with

beta-mercaptoethanol as a reducing agent. For F and G proteins, 100 ng was loaded per lane. Samples were heated at 95°C for 5 min. Samples were then loaded onto a 4–15% SDS-PAGE gel (Bio-Rad, Cat. No. 4561094). Proteins were transferred to PVDF membranes using the iBlot 3 dry blotting system (Invitrogen, Cat. No. IB1001) with iBlot 3 Transfer Stacks Mini PVDF (Invitrogen, Cat. No. IB34002), following the manufacturer's protocol. Membranes were briefly equilibrated in PBS, then blocked in 5% nonfat dry milk in TBST (TBS with 0.1% Tween-20) for 1 h at room temperature or overnight at 4°C with gentle shaking. Membranes were horizontally cut between 25 and 37 kDa to allow differential probing. The upper portion was probed with antibodies specific to RSV G (SinoBiological polyclonal rabbit anti-G Cat: 40041-T62 at 1:5,000) and RSV F (palivizumab at 1:5,000 and nirsevimab at 1:5,000), and the lower portion was probed with an anti–HIV-1 p24 antibody (Abcam ab32352 at 1:5,000) as a loading control for pseudovirus-containing samples. Primary antibodies were diluted in TBST with 5% nonfat dry milk and incubated with membranes for 1 h at room temperature. Blots were washed three times with TBST (0.2% Tween-20) for 5 min each, then incubated for 1 h at room temperature with a mix of HRP-conjugated secondary antibodies (anti-mouse HRP Millipore Sigma 710453, anti-rabbit HRP Invitrogen 31460, and anti-human HRP Bethyl Labs A80-104P each at 1:5,000) in TBST with 5% milk. After a second round of washes, membranes were rinsed in PBS. Signal was developed using a 1:1 mixture of ECL substrate and diluent (Super-Signal West Pico PLUS Chemiluminescent Substrate Thermo Protein Biology 34580) for 5 min and detected using a Bio-Rad imaging system. Western blot band intensities were quantified using the Gel Analysis tool in ImageJ (NIH). For each blot, the lanes corresponding to RSV F and G proteins and the corresponding HIV-1 p24 loading control were analyzed. Images were first converted to 8-bit grayscale, and the Gel Analyzer tool was used. Densitometric peaks were generated, and the area under the curve for each band was determined. For each lane, the intensity of the RSV F or G band was normalized to the corresponding p24 band to account for loading variation. The resulting values were reported as relative band intensity.

ACKNOWLEDGMENTS

We thank Richard Neher and Laura Urbanska for maintaining the public RSV Nextstrain build used for the phylogenetic trees in this paper. We thank Caleb Carr for assistance with the phylogenetic trees. The human sera from the 1980s are from the Infectious Disease Sciences Biospecimen Repository at the Vaccine and Infectious Disease Division (VIDD) of the Fred Hutchinson Cancer Center.

This work was funded by the NIH/NIAID under R01AI141707 (to J.D.B.) and 1U19AI181767 (subcontract to J.D.B.) and by the Gates Foundation under award INV-072143 (to J.D.B.). J.D.B. is an investigator at the Howard Hughes Medical Institute. C.A.L.S. is a fellow in the Pediatric Scientist Development Program. This project was supported by award number K12-HD000850 from the Eunice Kennedy Shriver National Institute of Child Health and Human Development. T.C.Y. was supported by an NSF graduate research fellowship (DGE-2140004). This research was supported by the Flow Cytometry Shared Resource (RRID:SCR_022613), of the Fred Hutch/University of Washington/Seattle Children's Cancer Consortium (P30 CA015704).

Conceptualization: C.A.L.S., T.E.M., and J.D.B. Methodology: C.A.L.S., T.E.M., J.D.B., X.J., T.C.Y., and N.B. Investigation: C.A.L.S. and T.E.M. Resources: X.J., T.C.Y., N.B., T.S.A., M.J.B., N.P.K., and A.L.G. Data curation: C.A.L.S., T.E.M., and J.D.B. Visualization: C.A.L.S., T.E.M., and J.D.B. Writing—Original Draft: C.A.L.S., T.E.M., and J.D.B. Writing—Review & Editing: C.A.L.S., T.E.M., X.J., T.C.Y., N.B., T.S.A., M.J.B., N.P.K., A.L.G., and J.D.B. Supervision: J.D.B. Funding Acquisition: C.A.L.S. and J.D.B.

AUTHOR AFFILIATIONS

[1]Basic Sciences and Computational Biology Divisions, Fred Hutchinson Cancer Center, Seattle, Washington, USA
[2]Department of Pediatrics, University of Washington, Seattle, Washington, USA

[3]Pediatric Infectious Diseases Division, Seattle Children's Hospital, Seattle, Washington, USA
[4]Molecular and Cellular Biology Graduate Program, University of Washington and Fred Hutch Cancer Center, Seattle, Washington, USA
[5]Department of Biochemistry, University of Washington, Seattle, Washington, USA
[6]Institute for Protein Design, University of Washington, Seattle, Washington, USA
[7]Vaccine and Infectious Disease Division, Fred Hutchinson Cancer Center, Seattle, Washington, USA
[8]Department of Laboratory Medicine and Pathology, University of Washington Medical Center, Seattle, Washington, USA
[9]Howard Hughes Medical Institute, Seattle, Washington, USA

AUTHOR ORCIDs

Cassandra A. L. Simonich http://orcid.org/0000-0001-6100-4652
Teagan E. McMahon http://orcid.org/0009-0008-4215-4717
Xiaohui Ju http://orcid.org/0000-0002-9552-0222
Terry Stevens-Ayers http://orcid.org/0000-0002-7546-8439
Michael J. Boeckh http://orcid.org/0000-0003-1538-7984
Alexander L. Greninger http://orcid.org/0000-0002-7443-0527
Jesse D. Bloom http://orcid.org/0000-0003-1267-3408

FUNDING

Funder	Grant(s)	Author(s)
National Science Foundation	DGE-2140004	Timothy C. Yu
National Institutes of Health	1U19AI181767	Jesse D. Bloom
National Institutes of Health	K12-HD000850	Cassandra A. L. Simonich
National Institutes of Health	R01AI141707	Jesse D. Bloom
Howard Hughes Medical Institute	Investigator	Jesse D. Bloom
Bill and Melinda Gates Foundation	INV-072143	Jesse D. Bloom

AUTHOR CONTRIBUTIONS

Cassandra A. L. Simonich, Conceptualization, Data curation, Formal analysis, Funding acquisition, Investigation, Methodology, Resources, Validation, Visualization, Writing – original draft, Writing – review and editing | Teagan E. McMahon, Conceptualization, Data curation, Formal analysis, Investigation, Methodology, Validation, Visualization, Writing – original draft, Writing – review and editing | Xiaohui Ju, Methodology, Resources, Visualization, Writing – review and editing | Timothy C. Yu, Methodology, Resources, Writing – review and editing | Natalie Brunette, Resources | Terry Stevens-Ayers, Resources | Michael J. Boeckh, Resources | Neil P. King, Resources | Alexander L. Greninger, Resources, Writing – review and editing | Jesse D. Bloom, Conceptualization, Data curation, Formal analysis, Funding acquisition, Methodology, Resources, Software, Supervision, Visualization, Writing – review and editing

DATA AVAILABILITY

We recommend readers visit https://github.com/jbloomlab/RSV-evolution-neut for well-documented links to visualizations and raw data. The full computational analysis of the neutralization data is available on GitHub repository at https://github.com/jbloomlab/RSV-evolution-neut/tree/main/02_notebooks. Visualizations are available at https://jbloomlab.github.io/RSV-evolution-neut/ and https://github.com/jbloomlab/RSV-evolution-neut/tree/main/03_output. The fraction infectivities used to calculate serum neutralization curves are available at https://github.com/jbloomlab/

RSV-evolution-neut/tree/main/01_data. Interactive versions of the RSV F protein phylogenetic trees used in this study are at https://nextstrain.org/community/jbloom-lab/RSV-evolution-neut@main/RSV-A-F and https://nextstrain.org/community/jbloom-lab/RSV-evolution-neut@main/RSV-B-F.

ETHICS APPROVAL

The human sera from the 1980s are from the Infectious Disease Sciences Biospecimen Repository at the Vaccine and Infectious Disease Division (VIDD) of the Fred Hutchinson Cancer Center. These sera were collected from prospective bone marrow donors with approval from the Fred Hutch's Human Subjects Institutional Review Board. We obtained the human sera previously tested for RSV neutralizing titers using a live virus assay (64) from the University of Washington Laboratory Medicine with human subject exemption determination by the Fred Hutch's Human Subjects Institutional Review Board and not human subject research determination by the University of Washington Human Subjects Division. All sera are fully de-identified.

ADDITIONAL FILES

The following material is available online.

Supplemental Material

Supplemental material (JVI00531-25-s0001.pdf). Figures S1 to S12; Tables S1 and S2.

REFERENCES

1. Suh M, Movva N, Jiang X, Bylsma LC, Reichert H, Fryzek JP, Nelson CB. 2022. Respiratory syncytial virus is the leading cause of United States infant hospitalizations, 2009-2019: a study of the National (Nationwide) inpatient sample. J Infect Dis 226:S154–S163. https://doi.org/10.1093/infdis/jiac120
2. Mazur NI, Caballero MT, Nunes MC. 2024. Severe respiratory syncytial virus infection in children: burden, management, and emerging therapies. The Lancet 404:1143–1156. https://doi.org/10.1016/S0140-6736(24)01716-1
3. Wildenbeest JG, Lowe DM, Standing JF, Butler CC. 2024. Respiratory syncytial virus infections in adults: a narrative review. Lancet Respir Med 12:822–836. https://doi.org/10.1016/S2213-2600(24)00255-8
4. Havers FP, Whitaker M, Melgar M, Pham H, Chai SJ, Austin E, Meek J, Openo KP, Ryan PA, Brown C, et al. 2024. Burden of respiratory syncytial virus–associated hospitalizations in US adults, October 2016 to September 2023. JAMA Netw Open 7:e2444756. https://doi.org/10.1001/jamanetworkopen.2024.44756
5. Ackerson B, Tseng HF, Sy LS, Solano Z, Slezak J, Luo Y, Fischetti CA, Shinde V. 2019. Severe morbidity and mortality associated with respiratory syncytial virus versus influenza infection in hospitalized older adults. Clin Infect Dis 69:197–203. https://doi.org/10.1093/cid/ciy991
6. Ruckwardt TJ. 2023. The road to approved vaccines for respiratory syncytial virus. npj Vaccines 8:138. https://doi.org/10.1038/s41541-023-00734-7
7. Capella C, Chaiwatpongsakorn S, Gorrell E, Risch ZA, Ye F, Mertz SE, Johnson SM, Moore-Clingenpeel M, Ramilo O, Mejias A, Peeples ME. 2017. Prefusion F, postfusion F, G antibodies, and disease severity in infants and young children with acute respiratory syncytial virus infection. J Infect Dis 216:1398–1406. https://doi.org/10.1093/infdis/jix489
8. Ngwuta JO, Chen M, Modjarrad K, Joyce MG, Kanekiyo M, Kumar A, Yassine HM, Moin SM, Killikelly AM, Chuang G-Y, Druz A, Georgiev IS, Rundlet EJ, Sastry M, Stewart-Jones GBE, Yang Y, Zhang B, Nason MC, Capella C, Peeples ME, Ledgerwood JE, McLellan JS, Kwong PD, Graham BS. 2015. Prefusion F-specific antibodies determine the magnitude of RSV neutralizing activity in human sera. Sci Transl Med 7:309ra162. https://doi.org/10.1126/scitranslmed.aac4241
9. Mazur NI, Terstappen J, Baral R, Bardají A, Beutels P, Buchholz UJ, Cohen C, Crowe JE Jr, Cutland CL, Eckert L, et al. 2023. Respiratory syncytial virus prevention within reach: the vaccine and monoclonal antibody landscape. Lancet Infect Dis 23:e2–e21. https://doi.org/10.1016/S1473-3099(22)00291-2
10. Walsh EE, Pérez Marc G, Zareba AM, Falsey AR, Jiang Q, Patton M, Polack FP, Llapur C, Doreski PA, Ilangovan K, et al. 2023. Efficacy and Safety of a Bivalent RSV Prefusion F Vaccine in Older Adults. N Engl J Med 388:1465–1477. https://doi.org/10.1056/NEJMoa2213836
11. Papi A, Ison MG, Langley JM, Lee D-G, Leroux-Roels I, Martinon-Torres F, Schwarz TF, van Zyl-Smit RN, Campora L, Dezutter N, de Schrevel N, Fissette L, David M-P, Van der Wielen M, Kostanyan L, Hulstrøm V, AReSVi-006 Study Group. 2023. Respiratory syncytial virus prefusion F protein vaccine in older adults. N Engl J Med 388:595–608. https://doi.org/10.1056/NEJMoa2209604
12. Wilson E, Goswami J, Baqui AH, Doreski PA, Perez-Marc G, Zaman K, Monroy J, Duncan CJA, Ujiie M, Rämet M, et al. 2023. Efficacy and safety of an mRNA-Based RSV PreF vaccine in older adults. N Engl J Med 389:2233–2244. https://doi.org/10.1056/NEJMoa2307079
13. Griffin MP, Yuan Y, Takas T, Domachowske JB, Madhi SA, Manzoni P, Simões EAF, Esser MT, Khan AA, Dubovsky F, Villafana T, DeVincenzo JP, Nirsevimab Study Group. 2020. Single-dose nirsevimab for prevention of RSV in preterm infants. N Engl J Med 383:415–425. https://doi.org/10.1056/NEJMoa1913556
14. Buchwald AG, Graham BS, Traore A, Haidara FC, Chen M, Morabito K, Lin BC, Sow SO, Levine MM, Pasetti MF, Tapia MD. 2021. Respiratory Syncytial Virus (RSV) neutralizing antibodies at birth predict protection from RSV illness in infants in the first 3 months of life. Clin Infect Dis 73:e4421–e4427. https://doi.org/10.1093/cid/ciaa648
15. Taleb SA, Al-Ansari K, Nasrallah GK, Elrayess MA, Al-Thani AA, Derrien-Colemyn A, Ruckwardt TJ, Graham BS, Yassine HM. 2021. Level of maternal respiratory syncytial virus (RSV) F antibodies in hospitalized children and correlates of protection. Int J Infect Dis 109:56–62. https://doi.org/10.1016/j.ijid.2021.06.015
16. Moline HL, Tannis A, Toepfer AP, Williams JV, Boom JA, Englund JA, Halasa NB, Staat MA, Weinberg GA, Selvarangan R, et al. 2024. Early estimate of nirsevimab effectiveness for prevention of respiratory syncytial virus-associated hospitalization among infants entering their first respiratory syncytial virus season - new vaccine surveillance network, October 2023-February 2024. MMWR Morb Mortal Wkly Rep 73:209–214. https://doi.org/10.15585/mmwr.mm7309a4
17. Kampmann B, Madhi SA, Munjal I, Simões EAF, Pahud BA, Llapur C, Baker J, Pérez Marc G, Radley D, Shittu E, et al. 2023. Bivalent prefusion F vaccine in pregnancy to prevent RSV illness in infants. N Engl J Med 388:1451–1464. https://doi.org/10.1056/NEJMoa2216480

18. CDC. 2025. RSV vaccine guidance for older adults. Respiratory syncytial virus infection (RSV). Available from: https://www.cdc.gov/rsv/hcp/vaccine-clinical-guidance/older-adults.html
19. Fleming-Dutra KE, Jones JM, Roper LE, Prill MM, Ortega-Sanchez IR, Moulia DL, Wallace M, Godfrey M, Broder KR, Tepper NK, Brooks O, Sánchez PJ, Kotton CN, Mahon BE, Long SS, McMorrow ML. 2023. Use of the pfizer respiratory syncytial virus vaccine during pregnancy for the prevention of respiratory syncytial virus-associated lower respiratory tract disease in infants: recommendations of the advisory committee on immunization practices - United States, 2023. MMWR Morb Mortal Wkly Rep 72:1115–1122. https://doi.org/10.15585/mmwr.mm7241e1
20. Jones JM, Fleming-Dutra KE, Prill MM, Roper LE, Brooks O, Sánchez PJ, Kotton CN, Mahon BE, Meyer S, Long SS, McMorrow ML. 2023. Use of nirsevimab for the prevention of respiratory syncytial virus disease among infants and young children: recommendations of the advisory committee on immunization practices — United States, 2023. MMWR Morb Mortal Wkly Rep 72:920–925. https://doi.org/10.15585/mmwr.mm7234a4
21. American Academy of Pediatrics (AAP). 2024. AAP recommendations for the prevention of RSV disease in infants and children. Available from: https://publications.aap.org/redbook/resources/25379/AAP-Recommendations-for-the-Prevention-of-RSV
22. Zhu Q, McLellan JS, Kallewaard NL, Ulbrandt ND, Palaszynski S, Zhang J, Moldt B, Khan A, Svabek C, McAuliffe JM, Wrapp D, Patel NK, Cook KE, Richter BWM, Ryan PC, Yuan AQ, Suzich JA. 2017. A highly potent extended half-life antibody as a potential RSV vaccine surrogate for all infants. Sci Transl Med 9:eaaj1928. https://doi.org/10.1126/scitranslmed.aaj1928
23. Sumsuzzman DM, Wang Z, Langley JM, Moghadas SM. 2025. Real-world effectiveness of nirsevimab against respiratory syncytial virus disease in infants: a systematic review and meta-analysis. Lancet Child Adolesc Health 9:393–403. https://doi.org/10.1016/S2352-4642(25)00093-8
24. Health Alert Network (HAN) - 00499. n.d. Limited availability of nirsevimab in the United States—interim CDC recommendations to protect infants from respiratory syncytial virus (RSV) during the 2023–2024 respiratory virus season. Available from: https://www.cdc.gov/han/2023/han00499.html
25. Terstappen J, Hak SF, Bhan A, Bogaert D, Bont LJ, Buchholz UJ, Clark AD, Cohen C, Dagan R, Feikin DR, et al. 2024. The respiratory syncytial virus vaccine and monoclonal antibody landscape: the road to global access. Lancet Infect Dis 24:e747–e761. https://doi.org/10.1016/S1473-3099(24)00455-9
26. Han AX, de Jong SPJ, Russell CA. 2023. Co-evolution of immunity and seasonal influenza viruses. Nat Rev Microbiol 21:805–817. https://doi.org/10.1038/s41579-023-00945-8
27. Cromer D, Reynaldi A, Mitchell A, Schlub TE, Juno JA, Wheatley AK, Kent SJ, Khoury DS, Davenport MP. 2024. Predicting COVID-19 booster immunogenicity against future SARS-CoV-2 variants and the benefits of vaccine updates. Nat Commun 15:8395. https://doi.org/10.1038/s41467-024-52194-9
28. Jian F, Wec AZ, Feng L, Yu Y, Wang L, Wang P, Yu L, Wang J, Hou J, et al. 2024. A generalized framework to identify SARS-CoV-2 broadly neutralizing antibodies. bioRxiv. https://doi.org/10.1101/2024.04.16.589454
29. Liu L, Iketani S, Guo Y, Chan JF-W, Wang M, Liu L, Luo Y, Chu H, Huang Y, Nair MS, Yu J, Chik KK-H, Yuen TT-T, Yoon C, To KK-W, Chen H, Yin MT, Sobieszczyk ME, Huang Y, Wang HH, Sheng Z, Yuen K-Y, Ho DD. 2022. Striking antibody evasion manifested by the Omicron variant of SARS-CoV-2. Nature 602:676–681. https://doi.org/10.1038/s41586-021-04388-0
30. Kistler KE, Bedford T. 2023. An atlas of continuous adaptive evolution in endemic human viruses. Cell Host Microbe 31:1898–1909. https://doi.org/10.1016/j.chom.2023.09.012
31. Hause AM, Henke DM, Avadhanula V, Shaw CA, Tapia LI, Piedra PA. 2017. Sequence variability of the respiratory syncytial virus (RSV) fusion gene among contemporary and historical genotypes of RSV/A and RSV/B. PLOS ONE 12:e0175792. https://doi.org/10.1371/journal.pone.0175792
32. Wilkins D, Langedijk AC, Lebbink RJ, Morehouse C, Abram ME, Ahani B, Aksyuk AA, Baraldi E, Brady T, Chen AT, et al. 2023. Nirsevimab binding-site conservation in respiratory syncytial virus fusion glycoprotein worldwide between 1956 and 2021: an analysis of observational study sequencing data. Lancet Infect Dis 23:856–866. https://doi.org/10.1016/S1473-3099(23)00062-2
33. Zhu Q, Patel NK, McAuliffe JM, Zhu W, Wachter L, McCarthy MP, Suzich JA. 2012. Natural polymorphisms and resistance-associated mutations in the fusion protein of respiratory syncytial virus (RSV): effects on RSV susceptibility to palivizumab. J Infect Dis 205:635–638. https://doi.org/10.1093/infdis/jir790
34. Simões EAF, Forleo-Neto E, Geba GP, Kamal M, Yang F, Cicirello H, Houghton MR, Rideman R, Zhao Q, Benvin SL, Hawes A, Fuller ED, Wloga E, Pizarro JMN, Munoz FM, Rush SA, McLellan JS, Lipsich L, Stahl N, Yancopoulos GD, Weinreich DM, Kyratsous CA, Sivapalasingam S. 2021. Suptavumab for the prevention of medically attended respiratory syncytial virus infection in preterm infants. Clin Infect Dis 73:e4400–e4408. https://doi.org/10.1093/cid/ciaa951
35. Zhu Q, Lu B, McTamney P, Palaszynski S, Diallo S, Ren K, Ulbrandt ND, Kallewaard N, Wang W, Fernandes F, Wong S, Svabek C, Moldt B, Esser MT, Jing H, Suzich JA. 2018. Prevalence and significance of substitutions in the fusion protein of respiratory syncytial virus resulting in neutralization escape from antibody MEDI8897. J Infect Dis 218:572–580. https://doi.org/10.1093/infdis/jiy189
36. Ahani B, Tuffy KM, Aksyuk AA, Wilkins D, Abram ME, Dagan R, Domachowske JB, Guest JD, Ji H, Kushnir A, Leach A, Madhi SA, Mankad VS, Simões EAF, Sparklin B, Speer SD, Stanley AM, Tabor DE, Hamrén UW, Kelly EJ, Villafana T. 2023. Molecular and phenotypic characteristics of RSV infections in infants during two nirsevimab randomized clinical trials. Nat Commun 14:4347. https://doi.org/10.1038/s41467-023-40057-8
37. Lin G-L, Drysdale SB, Snape MD, O'Connor D, Brown A, MacIntyre-Cockett G, Mellado-Gomez E, de Cesare M, Bonsall D, Ansari MA, et al. 2021. Distinct patterns of within-host virus populations between two subgroups of human respiratory syncytial virus. Nat Commun 12:5125. https://doi.org/10.1038/s41467-021-25265-4
38. Tabor DE, Fernandes F, Langedijk AC, Wilkins D, Lebbink RJ, Tovchigrechko A, Ruzin A, Kragten-Tabatabaie L, Jin H, Esser MT, Bont LJ, Abram ME, INFORM-RSV Study Group. 2020. Global molecular epidemiology of respiratory syncytial virus from the 2017-2018 INFORM-RSV study. J Clin Microbiol 59:e01828-20. https://doi.org/10.1128/JCM.01828-20
39. LuBLiu H, Tabor DE, Tovchigrechko A, Qi Y, Ruzin A, Esser MT, Jin H. 2019. Emergence of new antigenic epitopes in the glycoproteins of human respiratory syncytial virus collected from a US surveillance study, 2015-17. Sci Rep 9:3898. https://doi.org/10.1038/s41598-019-40387-y
40. Pandya MC, Callahan SM, Savchenko KG, Stobart CC. 2019. A contemporary view of Respiratory Syncytial Virus (RSV) biology and strain-specific differences. Pathogens 8:67. https://doi.org/10.3390/pathogens8020067
41. Raghunandan R, Higgins D, Hosken N. 2021. RSV neutralization assays - Use in immune response assessment. Vaccine (Auckl) 39:4591–4597. https://doi.org/10.1016/j.vaccine.2021.06.016
42. Gias E, Nielsen SU, Morgan LAF, Toms GL. 2008. Purification of human respiratory syncytial virus by ultracentrifugation in iodixanol density gradient. J Virol Methods 147:328–332. https://doi.org/10.1016/j.jviromet.2007.09.013
43. Bilawchuk LM, Griffiths CD, Jensen LD, Elawar F, Marchant DJ. 2017. The susceptibilities of respiratory syncytial virus to nucleolin receptor blocking and antibody neutralization are dependent upon the method of virus purification. Viruses 9:207. https://doi.org/10.3390/v9080207
44. Ausar SF, Rexroad J, Frolov VG, Look JL, Konar N, Middaugh CR. 2005. Analysis of the thermal and pH stability of human respiratory syncytial virus. Mol Pharm 2:491–499. https://doi.org/10.1021/mp0500465
45. Liljeroos L, Krzyzaniak MA, Helenius A, Butcher SJ. 2013. Architecture of respiratory syncytial virus revealed by electron cryotomography. Proc Natl Acad Sci USA 110:11133–11138. https://doi.org/10.1073/pnas.1309070110
46. Gupta CK, Leszczynski J, Gupta RK, Siber GR. 1996. Stabilization of respiratory syncytial virus (RSV) against thermal inactivation and freeze-thaw cycles for development and control of RSV vaccines and immune globulin. Vaccine (Auckl) 14:1417–1420. https://doi.org/10.1016/s0264-410x(96)00096-5
47. Caidi H, Harcourt JL, Haynes LM. 2016. RSV growth and quantification by microtitration and qRT-PCR assays. Methods Mol Biol 1442:13–32. https://doi.org/10.1007/978-1-4939-3687-8_2
48. Wang Y. 2023. Pseudotyped viruses. Springer Singapore Pte. Limited, Singapore.

49. Cantoni D, Wilkie C, Bentley EM, Mayora-Neto M, Wright E, Scott S, Ray S, Castillo-Olivares J, Heeney JL, Mattiuzzo G, Temperton NJ. 2023. Correlation between pseudotyped virus and authentic virus neutralisation assays, a systematic review and meta-analysis of the literature. Front Immunol 14:1184362. https://doi.org/10.3389/fimmu.2023.1184362
50. Cui G, Liu H, Li X, Ming L. 2020. Preliminary functional and phylogeographic analyses of the 72 nucleotide duplication region in the emerging human respiratory syncytial virus ON1 strain attachment glycoprotein gene. Biomed Pharmacother 123:109800. https://doi.org/10.1016/j.biopha.2019.109800
51. Hu L, Jiang J, Tang Y, Mei L, Wu L, Li L, Chen H, Long F, Xiao J, Peng T. 2023. A pseudovirus-based entry assay to evaluate neutralizing activity against respiratory syncytial virus. Viruses 15:1548. https://doi.org/10.3390/v15071548
52. Haid S, Grethe C, Bankwitz D, Grunwald T, Pietschmann T. 2016. Identification of a human respiratory syncytial virus cell entry inhibitor by using a novel lentiviral pseudotype system. J Virol 90:3065–3073. https://doi.org/10.1128/JVI.03074-15
53. Haid S, Grethe C, Bankwitz D, Grunwald T, Pietschmann TC for H. 2020. Correction for Haid et al., "identification of a human respiratory syncytial virus cell entry inhibitor by using a novel lentiviral pseudotype system". J Virol 94:e01690-19. https://doi.org/10.1128/JVI.01690-19
54. Crawford KHD, Eguia R, Dingens AS, Loes AN, Malone KD, Wolf CR, Chu HY, Tortorici MA, Veesler D, Murphy M, Pettie D, King NP, Balazs AB, Bloom JD. 2020. Protocol and reagents for pseudotyping lentiviral particles with SARS-CoV-2 spike protein for neutralization assays. Viruses 12:513. https://doi.org/10.3390/v12050513
55. Khetawat D, Broder CC. 2010. A functional henipavirus envelope glycoprotein pseudotyped lentivirus assay system. Virol J 7:312. https://doi.org/10.1186/1743-422X-7-312
56. Witting SR, Vallanda P, Gamble AL. 2013. Characterization of a third generation lentiviral vector pseudotyped with Nipah virus envelope proteins for endothelial cell transduction. Gene Ther 20:997–1005. https://doi.org/10.1038/gt.2013.23
57. Larsen BB, McMahon T, Brown JT, Wang Z, Radford CE, Crowe Jr JE, Veesler D, Bloom JD. 2024. Functional and antigenic landscape of the nipah virus receptor binding protein. bioRxiv. https://doi.org/10.1101/2024.04.17.589977
58. Yu J, Li Z, He X, Gebre MS, Bondzie EA, Wan H, Jacob-Dolan C, Martinez DR, Nkolola JP, Baric RS, Barouch DH. 2021. Deletion of the SARS-CoV-2 spike cytoplasmic tail increases infectivity in pseudovirus neutralization assays. J Virol 95:e00044-21. https://doi.org/10.1128/JVI.00044-21
59. Zhang H, Deng T, Fang Q, Li S, Gao S, Jiang W, Chen G, Yu K, Zhou L, Li T, Zheng Q, Yu H, Li S, Xia N, Gu Y. 2022. Endodomain truncation of the HIV-1 envelope protein improves the packaging efficiency of pseudoviruses. Virology (Auckl) 574:1–8. https://doi.org/10.1016/j.virol.2022.07.003
60. Crawford KHD, Dingens AS, Eguia R, Wolf CR, Wilcox N, Logue JK, Shuey K, Casto AM, Fiala B, Wrenn S, Pettie D, King NP, Greninger AL, Chu HY, Bloom JD. 2021. Dynamics of neutralizing antibody titers in the months after severe acute respiratory syndrome coronavirus 2 infection. J Infect Dis 223:197–205. https://doi.org/10.1093/infdis/jiaa618
61. Havranek KE, Jimenez AR, Acciani MD, Lay Mendoza MF, Reyes Ballista JM, Diaz DA, Brindley MA. 2020. SARS-CoV-2 spike alterations enhance pseudoparticle titers and replication-competent VSV-SARS-CoV-2 virus. Viruses 12:1465. https://doi.org/10.3390/v12121465
62. Sun Y, López CB. 2016. Preparation of respiratory syncytial virus with high or low content of defective viral particles and their purification from viral stocks. BIO Protoc 6:e1820. https://doi.org/10.21769/BioProtoc.1820
63. Moller-Tank S, Kondratowicz AS, Davey RA, Rennert PD, Maury W. 2013. Role of the phosphatidylserine receptor TIM-1 in enveloped-virus entry. J Virol 87:8327–8341. https://doi.org/10.1128/JVI.01025-13
64. Piliper EA, Reed JC, Greninger AL. 2024. Clinical validation of an RSV neutralization assay and analysis of cross-sectional sera associated with 2021-2023 RSV outbreaks to investigate the immunity debt hypothesis. Microbiol Spectr 12:e0211524. https://doi.org/10.1128/spectrum.02115-24
65. McDonald JU, Rigsby P, Atkinson E, Engelhardt OG, Study Participants. 2020. Expansion of the 1st WHO international standard for antiserum to respiratory syncytial virus to include neutralisation titres against RSV subtype B: an international collaborative study. Vaccine (Auckl) 38:800–807. https://doi.org/10.1016/j.vaccine.2019.10.095
66. McDonald JU, Rigsby P, Dougall T, Engelhardt OG, Study Participants. 2018. Establishment of the first WHO international standard for antiserum to respiratory syncytial virus: report of an international collaborative study. Vaccine (Auckl) 36:7641–7649. https://doi.org/10.1016/j.vaccine.2018.10.087
67. Cortjens B, Yasuda E, Yu X, Wagner K, Claassen YB, Bakker AQ, van Woensel JBM, Beaumont T. 2017. Broadly reactive anti-respiratory syncytial virus g antibodies from exposed individuals effectively inhibit infection of primary airway epithelial cells. J Virol 91:e02357-16. https://doi.org/10.1128/JVI.02357-16
68. Kishko M, Catalan J, Swanson K, DiNapoli J, Wei C-J, Delagrave S, Chivukula S, Zhang L. 2020. Evaluation of the respiratory syncytial virus G-directed neutralizing antibody response in the human airway epithelial cell model. Virology (Auckl) 550:21–26. https://doi.org/10.1016/j.virol.2020.08.006
69. King T, Mejias A, Ramilo O, Peeples ME. 2021. The larger attachment glycoprotein of respiratory syncytial virus produced in primary human bronchial epithelial cultures reduces infectivity for cell lines. PLOS Pathog 17:e1009469. https://doi.org/10.1371/journal.ppat.1009469
70. Anderson LJ, Jadhao SJ, Paden CR, Tong S. 2021. Functional features of the respiratory syncytial virus G Protein. Viruses 13:1214. https://doi.org/10.3390/v13071214
71. Gilman MSA, Castellanos CA, Chen M, Ngwuta JO, Goodwin E, Moin SM, Mas V, Melero JA, Wright PF, Graham BS, McLellan JS, Walker LM. 2016. Rapid profiling of RSV antibody repertoires from the memory B cells of naturally infected adult donors. Sci Immunol 1:eaaj1879. https://doi.org/10.1126/sciimmunol.aaj1879
72. Hall CB, Walsh EE, Long CE, Schnabel KC. 1991. Immunity to and frequency of reinfection with respiratory syncytial virus. J Infect Dis 163:693–698. https://doi.org/10.1093/infdis/163.4.693
73. JOHNSON KM, BLOOM HH, MUFSON MA, CHANOCK RM. 1962. Natural reinfection of adults by respiratory syncytial virus. Possible relation to mild upper respiratory disease. N Engl J Med 267:68–72. https://doi.org/10.1056/NEJM196207122670204
74. Hall CB, Long CE, Schnabel KC. 2001. Respiratory syncytial virus infections in previously healthy working adults. Clin Infect Dis 33:792–796. https://doi.org/10.1086/322657
75. Eguia RT, Crawford KHD, Stevens-Ayers T, Kelnhofer-Millevolte L, Greninger AL, Englund JA, Boeckh MJ, Bloom JD. 2021. A human coronavirus evolves antigenically to escape antibody immunity. PLOS Pathog 17:e1009453. https://doi.org/10.1371/journal.ppat.1009453
76. Lasrado N, Collier A-RY, Hachmann NP, Miller J, Rowe M, Schonberg ED, Rodrigues SL, LaPiana A, Patio RC, Anand T, Fisher J, Mazurek CR, Guan R, Wagh K, Theiler J, Korber BT, Barouch DH. 2023. Neutralization escape by SARS-CoV-2 Omicron subvariant BA.2.86. Vaccine (Auckl) 41:6904–6909. https://doi.org/10.1016/j.vaccine.2023.10.051
77. Johnson S, Oliver C, Prince GA, Hemming VG, Pfarr DS, Wang SC, Dormitzer M, O'Grady J, Koenig S, Tamura JK, Woods R, Bansal G, Couchenour D, Tsao E, Hall WC, Young JF. 1997. Development of a humanized monoclonal antibody (MEDI-493) with potent in vitro and in vivo activity against respiratory syncytial virus. J Infect Dis 176:1215–1224. https://doi.org/10.1086/514115
78. The IMpact-RSV Study Group. 1998. Palivizumab, a humanized respiratory syncytial virus monoclonal antibody, reduces hospitalization from respiratory syncytial virus infection in high-risk infants. Pediatrics 102:531–537. https://doi.org/10.1542/peds.102.3.531
79. Aliprantis AO, Wolford D, Caro L, Maas BM, Ma H, Montgomery DL, Sterling LM, Hunt A, Cox KS, Vora KA, Roadcap BA, Railkar RA, Lee AW, Stoch SA, Lai E. 2021. A phase 1 randomized, double-blind, placebo-controlled trial to assess the safety, tolerability, and pharmacokinetics of a respiratory syncytial virus neutralizing monoclonal antibody MK-1654 in healthy adults. Clin Pharmacol Drug Dev 10:556–566. https://doi.org/10.1002/cpdd.883
80. Gilman MSA, Moin SM, Mas V, Chen M, Patel NK, Kramer K, Zhu Q, Kabeche SC, Kumar A, Palomo C, Beaumont T, Baxa U, Ulbrandt ND, Melero JA, Graham BS, McLellan JS. 2015. Characterization of a prefusion-specific antibody that recognizes a quaternary, cleavage-dependent epitope on the rsv fusion glycoprotein. PLOS Pathog 11:e1005035. https://doi.org/10.1371/journal.ppat.1005035
81. Corti D, Bianchi S, Vanzetta F, Minola A, Perez L, Agatic G, Guarino B, Silacci C, Marcandalli J, Marsland BJ, Piralla A, Percivalle E, Sallusto F, Baldanti F, Lanzavecchia A. 2013. Cross-neutralization of four paramyxoviruses by a human monoclonal antibody. Nature 501:439–443. https://doi.org/10.1038/nature12442

82. Mousa JJ, Kose N, Matta P, Gilchuk P, Crowe JE. 2017. A novel pre-fusion conformation-specific neutralizing epitope on the respiratory syncytial virus fusion protein. Nat Microbiol 2:16271. https://doi.org/10.1038/nmicrobiol.2016.271
83. Fulton BO, Sachs D, Beaty SM, Won ST, Lee B, Palese P, Heaton NS. 2015. Mutational analysis of measles virus suggests constraints on antigenic variation of the glycoproteins. Cell Rep 11:1331–1338. https://doi.org/10.1016/j.celrep.2015.04.054
84. Thyagarajan B, Bloom JD. 2014. The inherent mutational tolerance and antigenic evolvability of influenza hemagglutinin. Elife 3:e03300. https://doi.org/10.7554/eLife.03300
85. Greaney AJ, Welsh FC, Bloom JD. 2021. Co-dominant neutralizing epitopes make anti-measles immunity resistant to viral evolution. Cell Rep Med 2:100257. https://doi.org/10.1016/j.xcrm.2021.100257
86. Agoti CN, Mwihuri AG, Sande CJ, Onyango CO, Medley GF, Cane PA, Nokes DJ. 2012. Genetic relatedness of infecting and reinfecting respiratory syncytial virus strains identified in a birth cohort from rural Kenya. J Infect Dis 206:1532–1541. https://doi.org/10.1093/infdis/jis570
87. Falsey AR, Singh HK, Walsh EE. 2006. Serum antibody decay in adults following natural respiratory syncytial virus infection. J Med Virol 78:1493–1497. https://doi.org/10.1002/jmv.20724
88. Henderson FW, Collier AM, Clyde WA, Denny FW. 1979. Respiratory-syncytial-virus infections, reinfections and immunity. A prospective, longitudinal study in young children. N Engl J Med 300:530–534. https://doi.org/10.1056/NEJM197903083001004
89. Habibi MS, Jozwik A, Makris S, Dunning J, Paras A, DeVincenzo JP, de Haan CAM, Wrammert J, Openshaw PJM, Chiu C, Mechanisms of Severe Acute Influenza Consortium Investigators. 2015. Impaired Antibody-mediated protection and defective IgA B-Cell memory in experimental infection of adults with respiratory syncytial virus. Am J Respir Crit Care Med 191:1040–1049. https://doi.org/10.1164/rccm.201412-2256OC
90. Blunck BN, Aideyan L, Ye X, Avadhanula V, Ferlic-Stark L, Zechiedrich L, Gilbert BE, Piedra PA. 2021. A prospective surveillance study on the kinetics of the humoral immune response to the respiratory syncytial virus fusion protein in adults in Houston, Texas. Vaccine (Auckl) 39:1248–1256. https://doi.org/10.1016/j.vaccine.2021.01.045
91. Sacconnay L, De Smedt J, Rocha-Perugini V, Ong E, Mascolo R, Atas A, Vanden Abeele C, de Heusch M, De Schrevel N, David M-P, Bouzya B, Stobbelaar K, Vanloubbeeck Y, Delputte PL, Mallett CP, Dezutter N, Warter L. 2023. The RSVPreF3-AS01 vaccine elicits broad neutralization of contemporary and antigenically distant respiratory syncytial virus strains. Sci Transl Med 15:eadg6050. https://doi.org/10.1126/scitranslmed.adg6050
92. Topalidou X, Kalergis AM, Papazisis G. 2023. Respiratory syncytial virus vaccines: a review of the candidates and the approved vaccines. Pathogens 12:1259. https://doi.org/10.3390/pathogens12101259
93. McLellan JS, Chen M, Leung S, Graepel KW, Du X, Yang Y, Zhou T, Baxa U, Yasuda E, Beaumont T, Kumar A, Modjarrad K, Zheng Z, Zhao M, Xia N, Kwong PD, Graham BS. 2013. Structure of RSV fusion glycoprotein trimer bound to a prefusion-specific neutralizing antibody. Science 340:1113–1117. https://doi.org/10.1126/science.1234914
94. Johnson SM, McNally BA, Ioannidis I, Flano E, Teng MN, Oomens AG, Walsh EE, Peeples ME. 2015. Respiratory Syncytial Virus uses CX3CR1 as a receptor on primary human airway epithelial cultures. PLOS Pathog 11:e1005318. https://doi.org/10.1371/journal.ppat.1005318
95. Teng MN, Whitehead SS, Collins PL. 2001. Contribution of the respiratory syncytial virus G glycoprotein and its secreted and membrane-bound forms to virus replication in vitro and in vivo. Virology (Auckl) 289:283–296. https://doi.org/10.1006/viro.2001.1138
96. Griffiths CD, Bilawchuk LM, McDonough JE, Jamieson KC, Elawar F, Cen Y, Duan W, Lin C, Song H, Casanova J-L, Ogg S, Jensen LD, Thienpont B, Kumar A, Hobman TC, Proud D, Moraes TJ, Marchant DJ. 2020. IGF1R is an entry receptor for respiratory syncytial virus. Nature 583:615–619. https://doi.org/10.1038/s41586-020-2369-7
97. Tayyari F, Marchant D, Moraes TJ, Duan W, Mastrangelo P, Hegele RG. 2011. Identification of nucleolin as a cellular receptor for human respiratory syncytial virus. Nat Med 17:1132–1135. https://doi.org/10.1038/nm.2444
98. N. Loes A, Araceli L Tarabi R, Bloom J. 2024 Sequencing-based neutralization assay for influenza A virus v1. https://doi.org/10.17504/protocols.io.kqdg3xdmpg25/v1
99. Tang A, Chen Z, Cox KS, Su H-P, Callahan C, Fridman A, Zhang L, Patel SB, Cejas PJ, Swoyer R, Touch S, Citron MP, Govindarajan D, Luo B, Eddins M, Reid JC, Soisson SM, Galli J, Wang D, Wen Z, Heidecker GJ, Casimiro DR, DiStefano DJ, Vora KA. 2019. A potent broadly neutralizing human RSV antibody targets conserved site IV of the fusion glycoprotein. Nat Commun 10:4153. https://doi.org/10.1038/s41467-019-12137-1
100. Hadfield J, Megill C, Bell SM, Huddleston J, Potter B, Callender C, Sagulenko P, Bedford T, Neher RA. 2018. Nextstrain: real-time tracking of pathogen evolution. Bioinformatics 34:4121–4123. https://doi.org/10.1093/bioinformatics/bty407
101. Huang K, Lawlor H, Tang R, MacGill RS, Ulbrandt ND, Wu H. 2010. Recombinant respiratory syncytial virus F protein expression is hindered by inefficient nuclear export and mRNA processing. Virus Genes 40:212–221. https://doi.org/10.1007/s11262-010-0449-8
102. Ternette N, Stefanou D, Kuate S, Uberla K, Grunwald T. 2007. Expression of RNA virus proteins by RNA polymerase II dependent expression plasmids is hindered at multiple steps. Virol J 4:51. https://doi.org/10.1186/1743-422X-4-51
103. Dadonaite B, Crawford KHD, Radford CE, Farrell AG, Yu TC, Hannon WW, Zhou P, Andrabi R, Burton DR, Liu L, Ho DD, Chu HY, Neher RA, Bloom JD. 2023. A pseudovirus system enables deep mutational scanning of the full SARS-CoV-2 spike. Cell 186:1263–1278. https://doi.org/10.1016/j.cell.2023.02.001
104. Matrosovich M, Matrosovich T, Carr J, Roberts NA, Klenk H-D. 2003. Overexpression of the alpha-2,6-sialyltransferase in MDCK cells increases influenza virus sensitivity to neuraminidase inhibitors. J Virol 77:8418–8425. https://doi.org/10.1128/jvi.77.15.8418-8425.2003
105. Hooper KA, Bloom JD. 2013. A mutant influenza virus that uses an N1 neuraminidase as the receptor-binding protein. J Virol 87:12531–12540. https://doi.org/10.1128/JVI.01889-13
106. Krarup A, Truan D, Furmanova-Hollenstein P, Bogaert L, Bouchier P, Bisschop IJM, Widjojoatmodjo MN, Zahn R, Schuitemaker H, McLellan JS, Langedijk JPM. 2015. A highly stable prefusion RSV F vaccine derived from structural analysis of the fusion mechanism. Nat Commun 6:8143. https://doi.org/10.1038/ncomms9143
107. Miroshnikov KA, Marusich EI, Cerritelli ME, Cheng N, Hyde CC, Steven AC, Mesyanzhinov VV. 1998. Engineering trimeric fibrous proteins based on bacteriophage T4 adhesins. Prot Eng Des Sel 11:329–332. https://doi.org/10.1093/protein/11.4.329
108. Loes AN, Tarabi RAL, Huddleston J, Touyon L, Wong SS, Cheng SMS, Leung NHL, Hannon WW, Bedford T, Cobey S, Cowling BJ, Bloom JD. 2024. High-throughput sequencing-based neutralization assay reveals how repeated vaccinations impact titers to recent human H1N1 influenza strains. J Virol 98:e0068924. https://doi.org/10.1128/jvi.00689-24